Macromolecules
ARTICLE

Macromolecules **2010**, *43*, 2389–2405 **2389**
DOI: 10.1021/ma902495z

Control of Structural Morphology in Shear-Induced Crystallization of Polymers

Oleksandr O. Mykhaylyk,*,† Pierre Chambon,†,‡ Ciro Impradice,†,§ J. Patrick A. Fairclough,† Nick J. Terrill,⊥ and Anthony J. Ryan†

†*Department of Chemistry, University of Sheffield, Sheffield, S3 7HF, U.K.,* ‡*Department of Chemistry, University of Liverpool, Crown Street, Liverpool,L69 7ZD, U.K.,* §*Department of Chemical and Food Engineering, University of Salerno, Via Ponte don Melillo, 84084 Fisciano, Italy, and* ⊥*Diamond Light Source Ltd, Diamond House, Didcot, OX11 0DE, U.K.*

Received November 11, 2009; Revised Manuscript Received January 29, 2010

ABSTRACT: Critical examination finds that the longest chains play a catalytic role in the formation of shish kebabs recruiting other chains into the formation of this morphology. The longest chains in an ensemble are stretched by shear flow to form the "shish" upon which the bulk of the material crystallizes as "kebabs". A universal parameter for the formation of shish kebab structures, the specific mechanical work, and a method by which it may be measured for any given ensemble of polymers is provided. In rotating parallel-plate flow a clear boundary is observed between oriented and unoriented material which is dependent on both the shear rate and the total strain. It has been found that the necessary conditions for the formation of oriented nuclei is that the shear rate should be larger than the inverse Rouse time of the longest chain in the ensemble and that mechanical work above a critical threshold is required. The experimental procedure required to make such measurements, and the precautions necessary to avoid artifacts such as elongated spherulites, elastic instabilities and photoelasticity, are examined in detail. The concept of the critical work being a control parameter has been previously demonstrated using model linear−linear hydrogenated polybutadiene blends and this concept is extended to industrial polymers, low-density polyethylene and polypropylene, using both small-angle X-ray scattering and polarized light imaging to measure orientation. The approach proposed is simple, is elegant, and can be easily implemented in the laboratory to study the fundamental processes of flow-induced crystallization and to test commercial materials before processing in real applications.

Introduction

It is well established that there are two dominant morphologies in semicrystalline polymers: spherulites and fibril-like shish kebabs. While the spherulites are a macroscopically isotropic structure of lamellae which form at quiescent conditions during crystallization from the melt, shish kebabs are anisotropic structures which can only be created under flow. The relative proportions of these two structures in the morphology of melt-processed polymers is one of the main factors responsible for the mechanical properties of industrial artifacts.[1] An enormous amount of information has been collected over the past decade which demonstrates that the formation of shish kebabs can be observed at relatively high flow rates, but, up to now there have been no clear criteria describing flow conditions required for the transition from spherulites or fringed micelles to the oriented morphologies of shish kebabs. For these reasons there was no theoretical guide as to how to control the flow during the processing of semicrystalline polymers to be able to create a precisely required morphology in molded or extruded products. Recent developments in shear-induced crystallization (SIC) have demonstrated the existence of boundary flow conditions for the onset of the oriented morphology, and more importantly, the parameters responsible for the formation of oriented shish kebab morphology have been identified.[2] It has been found that oriented (anisotropic) structures can only be formed if a polymer has experienced more than a threshold value of mechanical work performed on its melt, at shear rates, $\dot{\gamma}$, greater than the inverse Rouse time, τ_R, of the longest chains in the polymer ensemble ($\dot{\gamma} > 1/\tau_R$). It is not sufficient to perform the work if the shear rate is not above the critical value, and it is necessary that the threshold work is performed above this shear rate. Thus, there are two conditions which should be satisfied to produce an oriented shish kebab structure; the chains with a longer relaxation time in the polymer ensemble have to be *both* stretched by flow *and* delivered to each other to be able to form shish (oriented) nuclei upon which the bulk of the material could subsequently crystallize as kebabs.

The mechanism of the shish formation is still an open question. It could be a single event where a thread-like precursor grows out from the primary nuclei in the direction of flow[3] or an accumulation process where aggregation occurs, as soon as the number of point nuclei becomes large enough, resulting in a row of nuclei forming a shish.[4] In this work a generalizing term "shish nuclei" is used in the relation to the formation of oriented morphology. Despite this uncertainty, the general approach to flow-induced crystallization is still valid, as in both cases the formation of stable nuclei is required.

Shish structures can be thought to grow by the action of flow where a large number of low quality dormant nuclei are transformed into nuclei of a better quality, which are active at higher temperatures, following the long-established concept of dormant nuclei,[5] which is often either ignored or forgotten. Starting at the level of individual aggregates (dormant nuclei) this growth can lead to thread-like precursors initiating shish kebab structures.[5] This concept has been inspired by works[6,7] on the theory of

*Corresponding author. E-mail: O.Mykhaylyk@sheffield.ac.uk.

Published on Web 02/11/2010

nucleation, where it has been shown that the classical nucleation theory,[8] based on minimizing the Gibbs free energy of a liquid droplet by summation of the volume free energy and the surface free energy, does not allow for the occurrence of a stable nucleus of critical size. The stable nucleus should be formed in a step-by-step process. It has been suggested that the surface tension of a droplet is not a constant (i.e., independent of droplet size) at small sizes, which can result in the formation of stable molecular clusters with a radius considerably smaller than critical size estimated using classical theory. A coalescence of few of these small-but-stable clusters would suffice for the formation of an effective nucleus of a critical size for growth.[3] The question that arises is as follows: What would be a driving force for the formation of dormant nuclei (stable clusters) in polymer crystallization? One of possible answers is that stable dormant nuclei exist at all temperatures below the equilibrium melting point of the polymer.[5] However a systematic comparison of results on flow-induced crystallization,[9] recently underpinned by direct experimental observations,[2] suggests that stretching is a necessary condition for the formation of an oriented morphology. Thus, stretching of the molecules should be considered as the first step in the formation of shish nuclei which are created from dormant nuclei. These dormant nuclei have to be made stable and one possible reason for their stability under flow is that stretched segments of the coiled molecule reduce the configurational entropy of the chain allowing the stretched portions to come into closer contact with each other. A subsequent stabilization of the nuclei will occur when the structure possesses sufficient regularity. The longer the molecule the greater the number of stretched segments and, thereby, more intrachain contacts can be obtained potentially stabilizing the structure under certain flow conditions. Thus, long-chain molecules, with a large radius of gyration, are necessary in a polymer system for the formation of stable dormant nuclei. A dormant nucleus cannot survive without the flow as it may dissolve in the melt at quiescent conditions. However, while it has been created and stabilized under flow conditions (for example, during a step shear) it will collide with other dormant nuclei, where the number of collisions, facilitated by the mechanical work performed on the system during flow (a step shear), transforms low quality dormant nuclei into stable aggregate nuclei of a critical size to initiate shish formation. If the flow is stopped at this point, the aggregates formed, in contrast to separated dormant nuclei, will still be stable as their sizes are above the critical size of active nuclei required at these thermodynamic conditions. Aggregates possessing a size smaller than the critical size will dissolve. It is quite clear that the application of any mechanical action on the fluid will tremendously enhance the frequency of collisions and, therefore, the specific mechanical work[2,4,10] is an important parameter for the formation of aggregates. However, there is still a remaining question: either the dormant nuclei aggregate directly into fibrils forming stable elongated nuclei under flow conditions from the very beginning or the dormant nuclei aggregate into stable point nuclei first with further alignment of these point nuclei under flow into rows of nuclei transforming into the fibrillar morphology. Recent rheology measurements on shear-induced crystallization[11] suggest that point nuclei form first and then, after reaching a saturation point, transforms into another morphology corresponding to one-dimensional (fibrillar) structure. Thus, the whole scenario of the shish formation could be described as stretching of long molecules under flow conditions forming dormant nuclei, followed by collisions of the dormant nuclei under the flow creating stable point nuclei and, finally, alignment of the point nuclei into rows transforming into fibrillar structure.

Thermodynamic arguments further support this hypothesis. The interpretation above is nothing more than a particular case of the more general Willard Gibbs[12] concept of crystallization suggesting that the stability of a phase is related to the work that has to be done in order to create a critical nucleus of the new phase. This work can be either thermodynamic (heat) or mechanical work. In shear-induced crystallization some quantity of work is supplied to the system mechanically and not thermodynamically. As has been suggested previously[13] an additive term that accounts for the effect of the macroscopic flow on the free energy of the liquid phase has to be introduced $\Delta G = \Delta G_q + \Delta G_f$, where ΔG is the volumetric free energy difference between liquid and crystalline phase, ΔG_q is the component describing the change at quiescent conditions and ΔG_f is the component which should describe the effect of macroscopic flow incorporating both changes of the entropy required for the stabilization of dormant nuclei and the work performed on the system to aggregate the dormant nuclei forming stable shish nuclei.

The problem of flow-induced crystallization can be subdivided into extensional flow and shear flow. This work is dedicated to shear-induced crystallization; however, as has been discussed there will be no principle difference between the influences of mechanical work put into the sample either by shear flow or by extensional flow,[14] and the general conclusions derived from the results presented herein can be applied to phenomena observed in extensional flow geometry.

A Methodology for Shear-Induced Crystallization Measurements

Experiments on shear-induced crystallization require few important considerations before conducting measurements. These should include an optimization of the shear geometry to reduce the total time of the experiments and to increase sensitivity of the measurements, a selection of an instrument providing a necessary range of thermal and flow conditions to process polymers, and a choice of a temperature protocol based on thermal properties of the materials to be studied taking into account possible thermal history effects.

Shear Geometry. There are at least four different geometries often used in shear-induced orientation and crystallization studies: cone−plate,[15] rectilinear parallel plates (sandwich rheometer or sliding plates),[4,16] slot flow (duct flow),[17,18] and torsional parallel disks (rotating parallel plates).[2,19] While cone−plate geometry and rectilinear parallel plates produce a uniform shear rate across a sample both slot flow geometry and torsional parallel disks are characterized by a continuous variation of shear rates across the sample depending on the geometry of the device and the rheology of the material.[20] When the boundaries associated with different flow-induced processes have to be studied, in particular when the flow parameters controlling the formation of oriented structures are not known and need to be established, then geometries with a broad distribution of shear rates could be advantageous as they can be used in a combinatorial approach to detect the conditions necessary for the onset of oriented nuclei. Another advantage of slot flow and torsional parallel disks is that each point in the sample associated with different shear flow rate experiences the same temperature protocol, thus eliminating errors associated with the reproduction of temperature history possible with the repetition of the measurements required by the first group of geometries.

A boundary of transition between a spherulitic core and an oriented external layer can be clearly observed in polarized light images of polymers after SIC using pressure-driven slot flow geometry,[3,17] demonstrating that this geometry can be used in a combinatorial manner. However, the vector of the shear rate gradient perpendicular to the shear walls in this geometry complicates the measurements of the boundary

conditions when using either polarized light imaging (PI) or X-ray scattering methods.[21,22] Furthermore, control of the distribution of the shear rate in this geometry is complicated by the fact that the rheological properties of the material affect the distribution. The width of the slot is narrow and the gradient of the shear rate across the slot is usually high; these two factors significantly reduce the resolution of the measurements of the boundary conditions.

All of the problems associated with pressure driven flows can be solved with the radial distribution of shear rates in the torsional parallel disks geometry. The range of shear rates in this geometry can be easily adjusted with the angular speed. The vector of shear rate gradient is parallel to the shear disks, which provides an easy access to the parts of the samples experiencing different flow shear conditions, without damaging the sample. Thus, if moderate shear rates are required, the torsional parallel disks geometry is more efficient in the measurements of the boundary flow conditions for the formation of oriented structure.

Shear Instrument. There are two parameters which need a precise control by the instrument: the shear pulse (flow) and the temperature. At least two types of instruments with parallel disks geometry are readily available to perform measurements of critical parameters for the onset of oriented nuclei. These are commercial rheometers equipped with fixtures for parallel disks geometry and shear devices such as Linkam CSS 450 widely used in studies on shear-induced crystallization.[19,23−27] While rheometers provide a precise control of shear flow, a Linkam shear device with silver heating bodies offers better temperature control. However, relatively small samples would be required for shear experiments in a Linkam device in order to avoid a radial temperature gradient (the cell produces about 1 K drop in temperature at a radius 10 mm from the center).

The Linkam instrument requires some modifications to stabilize the performance of the motors and deal with normal forces, especially, for viscous materials. This problem has been resolved with an external high torque stepper motor (Pacific Scientific, T23NRHK-LDF-C5−00) attached to the cell and operated, in closed loop with an encoder, by intelligent controller (Pacific Scientific, PD2406-DI-001E) programmed from a computer.

Unloading of a sample from a shear instrument after SIC requires rigid fixtures (disks) which will not break when removing the sample from the instrument. Thus, the original glass disks supplied with a Linkam shear instrument may need to be replaced with metal analogues (steel disks have been used in this study).

Temperature-Shear Protocol. A typical experiment on shear-induced crystallization includes three important steps in the temperature protocol: melting of the polymer at temperatures high enough to remove memory of previous treatments (such as extrusion, hot-pressing, and so on), cooling the polymer down to the temperature where a shear pulse is applied to the melt followed by an isothermal crystallization and/or further cooling to a lower temperature to complete crystallization (Figure 1). Thus, there are a number of specific temperatures which have to be considered for the experiment. In this respect, discussion of a T, S-diagram showing the temperatures where several processes can occur, would be useful.[28] There is an upper (melting) transition corresponding to the equilibrium melting temperature (T_m^0) and a lower transition corresponding to the melting of spherulites (T_{ms}), often referred as a melting point of polymer. T_m^0 can be estimated from extrapolation methods[29,30] and should be associated with ideal crystals (i.e infinite and perfect crystals with complete crystallinity where

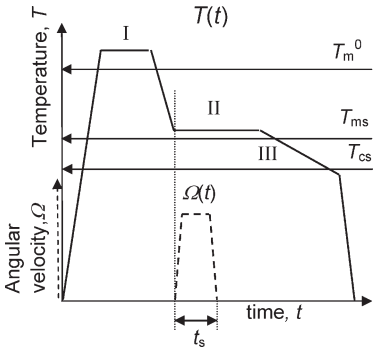

Figure 1. Shear-temperature protocol applied to the polymers during shear-induced crystallization. The temperature profile $T(t)$ (solid line) and the shear pulse for rotational geometry $\Omega(t)$ (dashed line) on a common time axis. Three stages of the protocol are shown: I polymer melting, II shear pulse, and isothermal treatment and III crystallization. Key: T_m^0, equilibrium melting point of the polymer; T_{ms}, end point of melting of spherulites; T_{cs}, peak temperature of crystallization of spherulites; t_s, the duration of the shear pulse.

structural imperfections such as fluctuations in the lamellar period caused by crystallization kinetics are absent), which are unlikely to be formed in sporadic nucleation taking place in crystallization of polymers from the melt. However, this temperature can be used as a guide temperature for melting (Figure 1, stage I) prior to shear-induced crystallization. A thermal treatment of the polymer above T_m^0 for sufficient time (i.e., much longer than disengagement time, τ_d, of the longest molecules in the polymer ensemble) will ensure that memory effects would be unlikely. The T_{ms} is associated with the melting temperature of polymers crystallized from the melt at quiescent conditions (semicrystalline polymers with a spherulitic morphology) and can be obtained from the melting curve using differential scanning calorimetry technique (DSC). At least four characteristic temperatures can be obtained from a DSC melting curves: the beginning of the melting, the extrapolated onset of the main endothermic peak, the peak temperature and the end of melting.[31] In this work, T_{ms} is related to the latter temperature.

In accordance with the T, S-diagram, there is a temperature range between T_m^0 and T_{ms} where thread-like precursors (shish nuclei), associated with an oriented (shish kebab) morphology forming under shear conditions, can be stable.[28] Thus, the shish nuclei are stable at higher temperatures than spherulitic forms and a melting temperature of the oriented morphology, i.e., the shish nuclei, has to be introduced, T_{mo}, to specify this difference. The enhanced thermal stability of oriented morphology has been recently reported for polyethylene where it has been observed by small-angle X-ray scattering (SAXS) methods that the melting temperature of shishes is 10 K higher than the melting temperature of spherulites and kebabs.[24] It is probably impossible to directly observe the initial formation of thread-like precursors (shish nuclei); they are present in such tiny proportions that rheology is not influenced to any extent and they are imperceptible in flow birefringence as the scattering power of the particles is proportional to the square of their volume.[4,10] Thus, direct measurements of temperature stability of shish nuclei (in particular T_{mo}) is difficult. In this respect, however, the memory effect can be exploited to analyze thermal stability of shish nuclei as their presence in a polymer melt influences the morphology of a crystallizing polymer. Shishes that are otherwise impossible to detect directly cause oriented crystallization of an apparently isotropic melt.

If the melting temperature of shish nuclei is above T_{ms} then these nuclei, created under flow conditions, should survive at

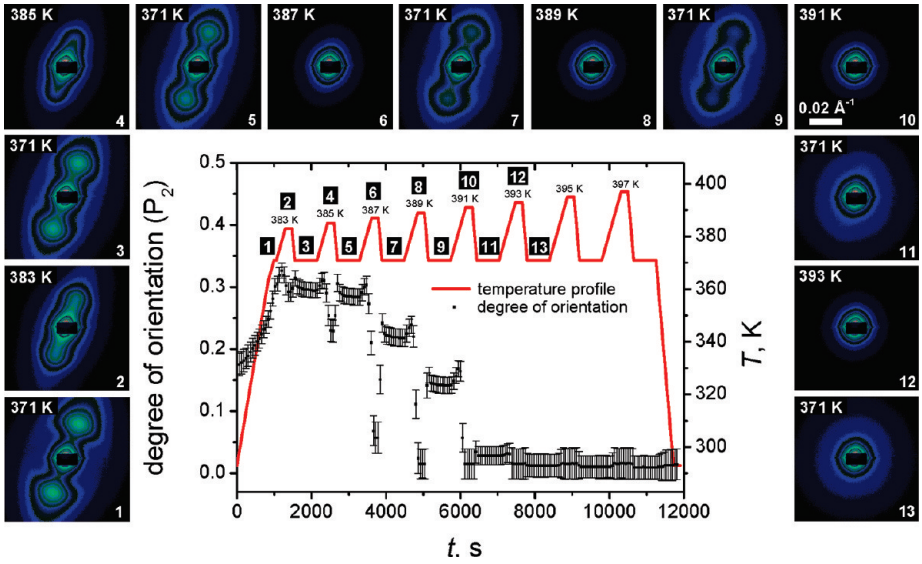

Figure 2. Detection of the melting point of oriented shish nuclei (T_{mo}) previously created in a polymer during shear-induced crystallization. The decrease of the degree of orientation (SAXS, SRS Daresbury Lab, station 2.1) with temperature is used to detect T_{mo} (filled symbols). Heat-treatment cycles are applied to a sample of a bimodal HPBD blend of 2 wt % 1.3 MDa in 15 KDa matrix, see Appendix, crystallized after shear pulse $\dot{\gamma} = 150\ s^{-1}$ for $t_s = 6.67$ s at 388 K and encapsulated in an aluminum DSC pan with mica windows. The heating protocol is steps of 2 K (383 K, 385 K and so on) alternated by cooling to below the temperature of spherulite crystallization (T_{cs}), 371 K. No orientation ($P_2 = 0$) is observed in the sample crystallized after heating to 393 K (pattern 13 and corresponding time−temperature range in the graph). The orientation of the lamellar stacking (SAXS) is parallel to the direction of the shear flow, applied at 388 K before crystallization. All of the SAXS patterns shown (1 - 13) have the same q scale (the scale bar is in the pattern number 10).

temperatures $T_{ms} < T < T_{mo}$ and act as oriented nucleating agents producing an oriented morphology on subsequent recrystallization. Formation of an oriented morphology (in particular, kebabs, detectable by X-ray techniques), replicating shish nuclei during crystallization, can be used to reveal shish nuclei in the polymer melt. Indeed, samples having an oriented morphology created by SIC have confirmed the stability of shish at higher temperatures (Figure 2). The SAXS patterns of the polymer melt recorded at temperatures above the melting of hydrogenated polybutadiene spherulites, $T_{ms} = 386$ K, (Figure 2, even-numbered patterns starting from number 6) show no orientation suggesting that the kebabs, representing the oriented morphology in the scattering patterns of crystalline material are in the melt state. However, cooling the melt to recrystallize the polymer still reveals the existence of an oriented structure even after melting at temperatures as high as 391 K (Figure 2, patterns 7, 9, and 11). It is only after melting at 393 K there is no orientation detectable in the recrystallized state (Figure 2, pattern 13). This suggests that heat treatments of the polymer at temperatures below 393 K do not erase oriented shish nuclei created in the polymer by SIC and, therefore, the melting temperature of shish nuclei in the studied material is between 391 K $< T_{mo} <$ 393 K. It could be argued that the changes observed in the orientation during temperature oscillations are a result of a time-dependent kinetic process and not a purely temperature-dependent phenomenon. However, similar measurements carried out with thermal cycles between 387 (melting) and 371 K (crystallization) for 36 000 s (10 h) have shown that such a long treatment at temperature above T_{ms} do not erase the shish nuclei. Furthermore, an experiment with the same range as described in the Figure 2, but using a temperature step of 4 K instead of 2 K (thereby halving the time at higher T), has revealed a similar result 391 K $< T_{mo} <$ 395 K. Thus, exploring the memory effects of oriented recrystallization shows that the shish nuclei can be stable at temperatures above the melting point of spherulites ($T_{mo} > T_{ms}$). Most probably, the temperature stability of shish nuclei is dependent on the regularity of the crystal structure and the crystal sizes controlled by the molecules involved in the shish formation during a shear flow.

The choice of the temperature protocol, such as melting and crystallization temperatures and the rate of cooling and heating, should be based on two important phenomena: the nucleation caused by shear flow and the nucleation caused by temperature. Both these processes contribute to the total crystallization. Since $T_{mo} > T_{ms}$, at least two different nucleation scenarios exist in shear-induced crystallization. If the shear pulse is applied to the polymer at temperatures above T_{ms} but below T_{mo} then only shish nuclei can be formed at this temperature, and during cooling at temperatures below T_{ms} kebabs will grow before spherulites can nucleate. Whereas SIC at temperatures below T_{ms} creates shish nuclei accompanied by the formation of spherulitic nuclei, where both work as nucleating agents for the remaining material: the first type of nuclei will cause a crystallization of the material in kebabs and the second type will cause crystallization of spherulites. The volume ratio of the material crystallized in either the shish kebab or spherulitic morphology will be dependent on the density of shish nuclei created by flow (controlled by flow parameters and temperature at which the shear flow has been performed), and on the rate of sperulitic nucleation during cooling. Thus, at slow cooling rates shish nuclei created during shear pulse will be a dominating factor in crystallization of the polymer, while at fast cooling rates heterogeneous nucleation and crystal growth of spherulites may compete with crystallization caused by shish nuclei. Performing SIC at temperatures above T_{ms} enables the shish nuclei formation to be separated from spherulitic nuclei and, thus, observe effect of the flow parameters on the nucleation of oriented morphology. If a shear flow experiment is performed at temperatures below T_{ms} then both shish nuclei, triggered by flow, and spherulitic nuclei, triggered by temperature, should be considered in the analysis. It is desirable, therefore, to carry out SIC experiments at temperatures above T_{ms} to avoid effects

of temperature-driven nucleation. The upper limit of the temperature for shearing is defined by the thermodynamic stability of shear-induced nuclei and can be detected experimentally from SAXS measurements (Figure 2). The T_{ms} temperature can be defined from DSC. The temperature gap between the melting point of spherulitic morphology of the polymer and the melting point of the shish depends on molecular structure. This gap is about 6 K for hydrogenated polybutadienes but it can be much bigger for isotactic polypropylenes.[28]

Following this discussion three time lags (heat soak intervals) have to be considered for a shear-temperature protocol to perform shear-induced crystallization (Figure 1):

I. After loading the material into the shear device, it should be heated up to a temperature above T_m^0 and the gap between plates in torsional shear geometry should be set; the sample should be kept at this temperature for a time much longer than τ_d of the longest molecules present in the polymer ensemble to erase all thermal and flow history and then be cooled to the required temperature at which the shear pulse should be performed.

II. In isothermal treatment, the duration of the lag should be longer than the duration of the shear pulse; since the oriented nuclei have been formed by the shear flow at temperatures above T_{ms}, the nuclei are thermodynamically stable and can persist for a long time (at least hours) at the shearing temperature.

III. For cooling the sample down to the crystallization temperature, slow rates should be used; fast cooling has to be avoided as it may affect the quality of the crystals and, therefore, the appearance of the structural orientation in PI or in SAXS; once past the spherulite crystallization temperature, T_{cs}, the sample has to be cooled to room temperature at a fast rate (to save time) and unloaded from the shear device.

Justification of the Method

Materials representing both polyethylenes and polypropylenes (see Appendix) have been chosen to demonstrate the existence of a boundary between oriented and unoriented morphologies during shear and to justify the method of the measurements of the boundary flow conditions. While some solid polymer microstructures are opaque to visible light making most optical methods inappropriate for detection of structure, the materials presented herein (LDPE, PP and in some cases HPBD) enable results obtained by both optical and X-ray scattering techniques to be compared (Figure 3). The conclusions drawn in this section, based on both techniques, can be widely applied to other semicrystalline polymers, when only one or other of the techniques would be necessary.

Two types of samples can be identified among polymer disks unloaded from a torsional parallel plate shear device after SIC. Homogenous samples which have been sheared at relatively small angular speeds for a relatively short time and have no orientation detected across the disks. Heterogeneous samples, which have experienced higher shear rates at higher angular speed and/or longer time of shearing, contain areas of oriented and unoriented morphology with a transition zone between. The latter samples are of the main interest of this study (Figure 3). Different analysis techniques show a correlation between features observed from the microstructure of the polymers created during shear (Figure 3, follow the blue arrows crossing the figure). The opaque central zone of the sample observed in the optical images (Figure 3, parts a and b) corresponds to the nonbirefringent central zone of the samples observed in the polarized light images (Figure 3, parts c and d) and the point where the degree of orientation (see Appendix), calculated from a radial SAXS scan of the samples, starts to grow (Figure 3, parts f and g). The central opaque zone is an area that has experienced little shear and contains objects that cause both multiple and isotropic scattering whereas the outer translucent zone has experienced high shear and thereby contains fewer structures that cause either isotropic and/or multiple scattering. The polarized light images of the samples show more strongly differentiated features with a clear boundary between the nonbirefringent central zone and the birefringent outer zone (Figure 3, parts c and d) resembling a conoscopic image of a uniaxial crystal.[32] The SAXS and WAXS patterns (Figure 3, parts c and d, SAXS and WAXS insets collected from the central and the outer zone of the samples) indicate that the outer zone of the sample has an oriented morphology, which resembles shish kebabs, and is typical for these polymers after SIC. The scattering patterns suggest that the central (unoriented) zone of PP corresponds to α-isotactic polypropylene (α-iPP). The oriented zone of PP is composed of two phases: α-iPP and γ-iPP (the latter is known to be formed in propylene−ethylene random copolymers[33] and also in uniaxially oriented iPP[34]), and has a typical crosshatched structural morphology (see 110_α in PP WAXS, Figure 3) with uniaxial orientation of the α-crystals about their *c*-axis (chain axis) preferably parallel to the flow direction.[22] The patterns of the LDPE correspond to polyethylene orthorhombic unit cell. The oriented zone of LDPE has a structure with lamellae twisted around crystallographic *b*-axes parallel to the radius vectors of the sample, similar to the radial orientation in a single spherulite. Consistent with the X-ray scattering data, the Maltese cross and fringes of Newton rings (spreading out with alternating colors toward the edge of the sample) indicate the birefringence of the material, with a boundary of truncation at the central zone of the sample originating from the oriented polymer structure. The pattern of the structural orientation of the sheared samples can be represented as a slice of a big spherulite with the core removed. Polyethylene forms negative sperulites with the long axes of the optical indicatrices of the twisted lamellae normal to the radius vector of the spherulite.[35] In analogy with the spherulites, the schematic diagram of polarizability ellipsoids, which are the superposition of the separate polarization optic indicatrices of the lamellae, can be drawn to represent birefringence of each segment of the LDPE sample (Figure 3e).

The appearance of the oriented structure in the sheared samples indicated by the increase of the P_2 function from a zero (Figure 3, parts f and g) coincides with the boundary between the birefringent and nonbirefringent zones of the samples. Thus, by performing a shear-induced crystallization and unloading the sample from the shear device the boundary between the oriented and unoriented zones can by detected by polarized light imaging and/or the P_2 function calculated from X-ray scattering patterns (see Appendix). Since the sheared samples have a radial symmetry, a SAXS scan across the diameter of the sample is sufficient to detect the radius of the boundary, r_b (Figure 3c−e). However, when the transparency of the sheared samples permits, measurements of r_b from two-dimensional polarized light images are more reliable and less-time-consuming as it records the whole image of the sample at once and requires simple equipment readily available in many laboratories. The observed boundaries are relatively sharp and imaging software can be used to measure their radius. There is an uncertainty of the boundary position caused by both deviations of the boundary from a circular shape and the resolution of the instrument used for the measurements. An error of 0.5 mm has been estimated in the r_b measurements in

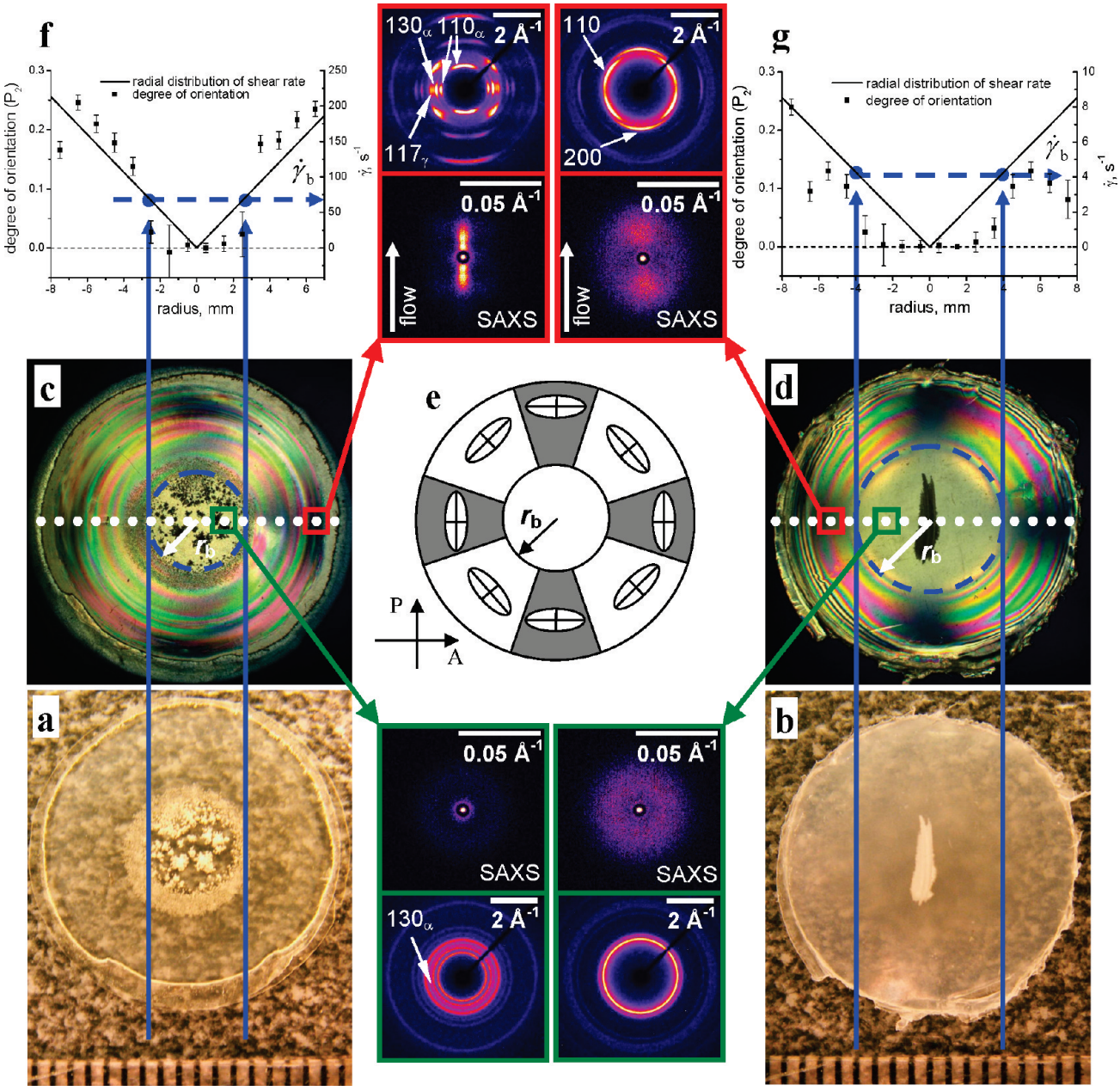

Figure 3. Structural analysis of two representative polymer samples, a propylene−ethylene random copolymer (left) and low-density polyethylene, Lupolen 1840H, (right) after shear-induced nucleation and subsequent crystallization (shear pulses $\Omega = 13.33$ rad/s for $t_s = 4$ s at $T = 433$ K and $\Omega = 0.53$ rad/s for $t_s = 4$ s at 385 K, respectively, torsional parallel disks, $d = 0.5$ mm). (a, b) optical images of the samples with a rule (mm scale). (c, d) polarized light images of the samples. (e) Schematic drawing of extinction directions in the sheared samples (the polarizability ellipsoids represent a superposition of optical indicatrices in the LDPE sample, the vectors labeled by letters P and A are a polarizer and an analyzer transmission azimuth, respectively) and (f, g) a corresponding plot of radial distribution of degree of lamellar orientation (grid lines corresponding to zero degree of orientation are shown) calculated from a SAXS scan of the sample along the diameter (along the white dashed line shown on c and d) overlapped with a plot of the shear rates experienced by the polymer. Insets show SAXS (Bruker Nanostar) and wide-angle X-ray scattering patterns, WAXS, corresponding to the oriented (red squares) and nonoriented (green squares) zones of the samples. Selective indexing of the WAXS patterns is shown. r_b (c and d) indicates the boundary between nonoriented and oriented morphology in the sheared samples and $\dot{\gamma}_b$ (f, g) indicates shear rate corresponding to the boundary ($\dot{\gamma}_b = \Omega r_b/d$).

the presented work. Since the distribution of the shear rates is know for the torsional disks geometry

$$\dot{\gamma}(t) = \frac{\Omega(t)r}{d} \qquad (1)$$

where $\Omega(t)$ is the angular speed of the rotating disk and d is the gap between the shear plates, the obtained radius of the boundary can be recalculated into the boundary shear rate, $\dot{\gamma}_b$ (Figure 3, parts f and g).

The $\Omega(t)$ and d parameters can be variable in the torsional disks geometry, but if their ratio is kept constant, with the rest of the parameters unchanged, the shear experiments should reproduce the same radius of the boundary of transition between oriented and unoriented material (Figure 4). An increase of the thickness of a sheared sample (controlled by the gap d), which increases retardation between ordinary and extraordinary beam can make the birefringence and, therefore, PI more sensitive for the detection of the boundary and the structural changes in the material (Figure 4, note the increase of the number of fringes

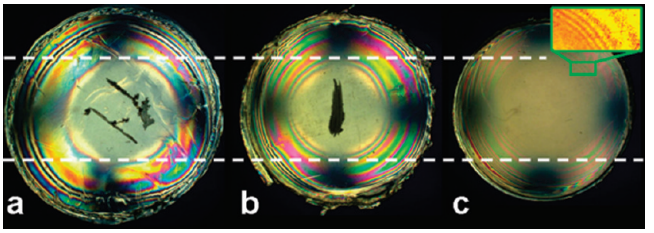

Figure 4. Polarized light images of the LDPE samples sheared at $T = 385$ K with different gap settings between the shearing plates [$d = 0.25$ mm (a), 0.5 mm (b), and 1.0 mm (c)] but with the same shear rate distribution through the samples: $\Omega = 0.252$ rad/s (a), 0.53 rad/s (b), and 1.06 rad/s (c) for $t_s = 4$ s. The guiding white dashed lines indicate boundary between unoriented and oriented parts of the samples. The width of the image strip is equivalent to 21 mm. The inset shows a zoomed contrast-adjusted boundary area of the sample c.

within the boundary proportional to the increase of the thickness of the sheared samples going from 1 in Figure 4a to 2 in Figure 4b and to 4 in Figure 4c). But an increase of the sample thickness also reduces the samples transparency for optical measurements (Figure 4a−c). There is, therefore, an optimal thickness and the sample should be thin enough to be at least translucent for a visible light and thick enough to retain the PI sensitivity. The thickness of a sample is also important for maintaining the circular shape of the sample during shear. It has been found that the 0.5 mm is a good starting point to perform initial measurements.

Since the radial distribution of shear rates across the sample is proportional to the angular speed, eq 1, a variation of the angular speed can be used to control the shear rate. An increase of the angular speed makes the range of shear rates accessible in the shear experiment wider, which is useful for finding boundary conditions for the formation of oriented morphology. A decrease of the angular speed narrows the range of shear rates at small values, which can increase the precision of the measurements of the boundary conditions. This also suggests that the radial position of the transition between oriented and unoriented morphology, r_b, detected from shear experiments performed at different angular speed with the same shear pulse duration, should be changed in a way that gives a constant shear rate associated with the boundary, $\dot{\gamma}_b$. Indeed, samples where SIC was performed at different angular velocities show a transition boundary at different radii (Figure 5, parts a and b) but corresponding to the same shear rate (Figure 5, parts a and b, follow the circles given for a guidance) provided the rest of the parameters remain constant. Plotting the degree of orientation versus shear rate, to scale both experiments to a comparable parameter, shows the same pattern reproducing similar features of the boundary between oriented and unoriented morphology (Figure 5c), even if the resolution of the first experiment within the transition zone is poor (Figure 5a). Thus, the results presented show that the boundary shear rate is a specific parameter characterizing the polymer in question, and is reproducible under different experimental conditions.

The key parameter associated with the formation of oriented morphology of a polymer is the specific work of flow experienced by the polymer during shear.[2] If analytical expressions of both the boundary shear rate $\dot{\gamma}_b(t)$ and the approximation of the viscosity $\eta[\dot{\gamma}_b(t)]$ are known then the integral of the boundary specific work can be calculated:

$$w_b = \int_0^{t_s} \eta[\dot{\gamma}_b(t)]\dot{\gamma}_b{}^2(t)\,dt \qquad (2)$$

Here t_s is the duration of shearing. If the analytical expressions are not known, then numerical integration has to be used. The total

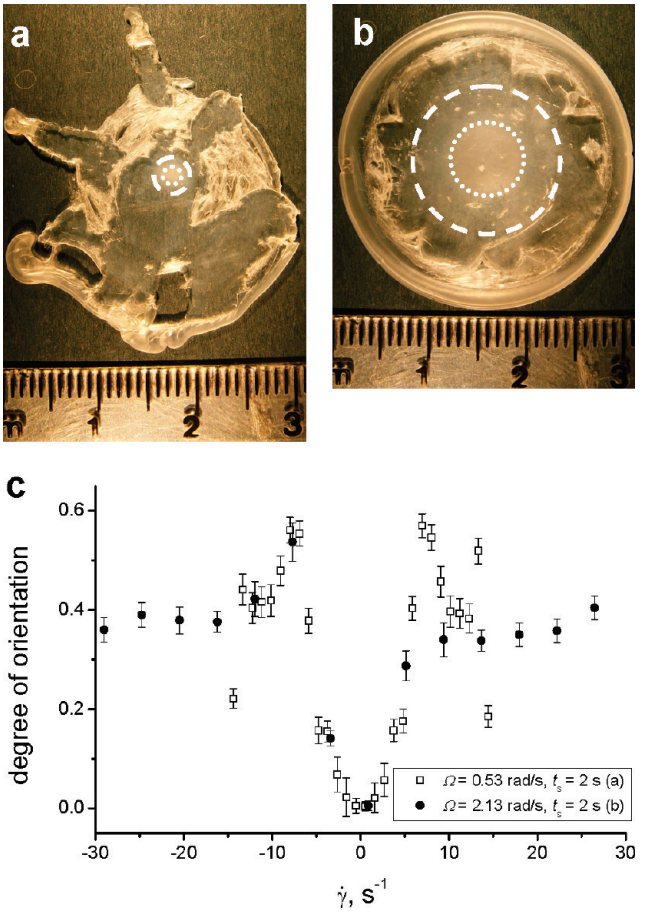

Figure 5. Optical images of the LDPE samples sheared at different angular speed [$\Omega = 2.13$ rad/s (a) and $\Omega = 0.53$ rad/s (b)] for the same duration $t_s = 2$ s, $T = 377$ K. Dotted and dashed lines, given for guidance, indicate circles of shear rates corresponding to 4 s^{-1} and 8 s^{-1}, respectively. Corresponding plots of the degree of orientation of the polymers measured (SAXS, Bruker Nanostar) along the diameter of the samples (c). The zero shear rate corresponds to the center of the sample, the negative values of the shear rate corresponds to the left-hand side of the samples and the positive to the right-hand side of the samples.

mechanical work experienced by a unit volume of the polymer during a shear pulse is represented in eq 2. When the viscosity of the polymer is high and/or a relatively high angular speed is applied in the experiment then an acceleration period, $\ddot{\gamma}(t)$, can be used to produce a trapezoidal pulse instead of a rectangular pulse; this reduces the overshoot caused by a nonlinear response of the polymer during start-up. It also helps to avoid damage to the sample during shear at high rates. In this case, the shear rates are not constant and the calculation of the specific work of flow requires integration over the total flow taking into account the dependence of polymer viscosity on the applied shear rates. If the shear pulse is of a rectangular shape and the acceleration time of the shear plates is negligible, then it can be assumed in the boundary specific work calculations, eq 2, that both the boundary shear rate and the viscosity are constant $\{\dot{\gamma}_b(t) = \dot{\gamma}_b$ and $\eta[\dot{\gamma}_b(t)] = \eta(\dot{\gamma}_b)\}$; therefore, the integration over the period of shearing t_s can be substituted by a simple multiplication of the parameters:

$$w_b = \eta(\dot{\gamma}_b)\dot{\gamma}_b^2 t_s \qquad (3)$$

There are a few structural effects which should be considered for the torsional parallel disks geometry. The polarized light images obtained (Figure 3, parts c and d) can be a result of a photoelastic effect caused by anisotropy of the refractive index

originating from residual strain. The isoclinic fringes represented by a truncated Maltese cross may correspond to the principal stress direction and the isochromatic circular fringes may correspond to the lines of constant principal stress difference. A flow-induced residual stress created during a shear pulse could be one of the causes of the birefringence.[36] However, even if solidification occurs after the polymer molecules are fully relaxed, which can be achieved by a long isothermal annealing at the shearing temperature (1 h has been used in this work for the samples sheared at temperatures above T_{ms}) the oriented shish nuclei created during shear will still produce a stress in the sample during crystallization. Since the distribution of the shear rates across the sample under shear has higher values at the edge of the sample, then the number of molecules in a stretched state and, subsequently, the probability of the formation of oriented nuclei at the edge of the sample are higher with a reduction of these values toward the central zone of the sample where no oriented nuclei are produced during shear. This higher density of nuclei causes a faster rate of crystallization creating an annulus of crystallized polymer with the crystallization front moving toward center of the sample. The molten center of the sample, confined by the shear disks, experiences a compression due to shrinkage of the solidified annulus. Thus, as the material crystallizes from the edge to the center of the sample the volume elements are under different packing pressures producing a radial distribution of stress in the crystallized sample. The pronounced circular fringe observed in PIs (Figure 6) is probably the result of a compensation of two forces originating from shrinkage of the crystallized polymer ring and compressibility of the polymer melt in the center of the sample. The location of this fringe can also be identified as a reproducible drop in the degree of orientation of the lamellar structure (Figure 6c, follow the blue arrows). This drop is probably caused by the local movement of the material during crystallization. Similar drop in the degree of orientation can be found in other shear experiments for LDPE samples sheared at temperatures above T_{ms} (Figure 3g) and below T_{ms} (Figure 5c). The less elastic PP does not show such a pronounced effect in either PI (Figure 3c) or the degree of orientation (Figure 3f), which suggests that this extra feature observed in the LDPE PI is of elastic origin.

Despite the residual strain in the crystallized samples complicating the observed PI, this effect is directly related to the concentration of oriented nuclei controlling the process of crystallization after shear pulse. Thus, lines of constant principal stress difference parallel to the flow direction controlling the lateral orientation of shish nuclei contribute to the total birefringence, amplifying the effect of oriented structure and the sensitivity of the PI measurements.

The Maltese cross observed in the central zone of the polarized light image (Figure 6b) could also be associated with the residual strain created during crystallization of the polymer after SIC. However, there is only a truncated Maltese cross with no extinction observed in the central part of the samples sheared at temperatures above the melting point of spherulites (Figure 3g). Thus, it is reasonable to suggest that the appearance of the Maltese cross in the central part of the samples sheared at temperatures below melting point of spherulites is a temperature-related phenomenon. One of the possible scenarios is that spherulitic nuclei, which are likely to appear at temperatures below T_{ms} in any zone of the sample, began to form during flow and were deformed by that flow resulting in an elongated spherulite morphology.[37,38] Such a morphology will create anisotropy in crystal orientation causing birefringence of the material resulting in Maltese cross. There is a good correlation between the features observed in PI (Figure 6b) and the degree of orientation measured from SAXS scan (Figure 6c). A slight increase of the degree of orientation in the central zone of the

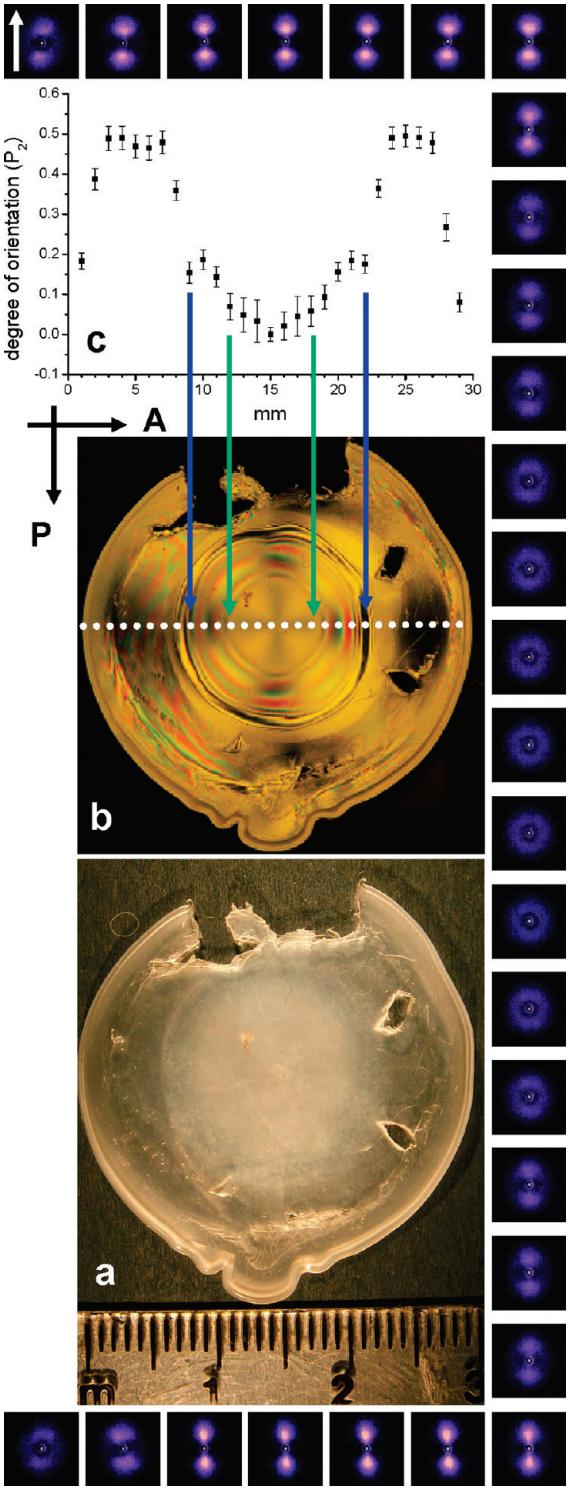

Figure 6. Structural analysis of an LDPE sample (Lupolen 1840H) unloaded from the shear device after shear-induced nucleation (Ω = 0.067 rad/s for t_s = 30 s at 377 K, d = 0.5 mm) and subsequent crystallization. (a) Optical image of the sample with a scale in mm, (b) a polarized light image of the sample (the vectors labeled with letters P and A show transmission azimuth of polarizer and analyzer, respectively), and (c) a plot of degree of lamellar orientation (P_2 function) obtained from SAXS scan (Bruker Nanostar) of the sample along its diameter (the white dots in part b show location of the points of the scan). The blue and green arrows relate orientation (c) to the radial positions in part b. SAXS patterns used for the calculation of degree of orientation surround the figure, starting at the top left image corresponding to the left most point in part b proceeding in a clockwise manner. The white arrow indicates the flow direction.

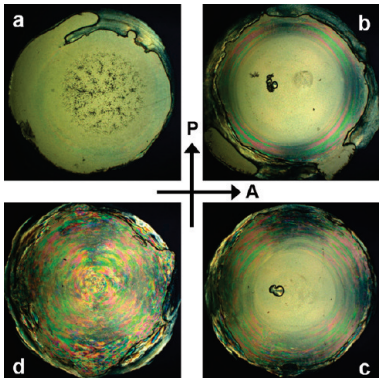

Figure 7. Polarized light images of propylene−ethylene random copolymer samples (crystallized after a shear pulse of $\Omega = 2.67$ rad/s for durations of $t_s = 10$ s (a), $t_s = 30$ s (b), $t_s = 50$ s (c), and $t_s = 100$ s (d) at 428 K), demonstrating the appearance of a secondary flow effect with increasing shear pulse duration. The length of each side of the images is equivalent to 18 mm. Two perpendicular vectors labeled with letters P and A show transmission azimuth of polarizer and analyzer, respectively.

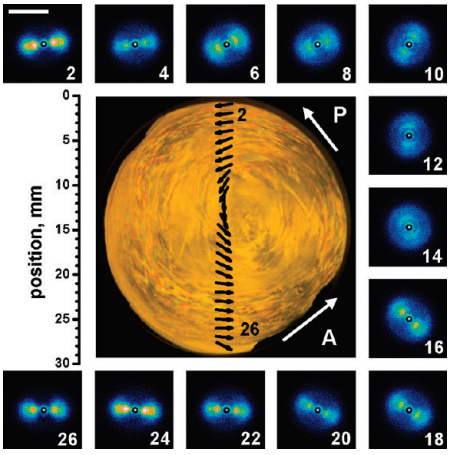

Figure 8. Polarized light image (PI) of a bimodal blend of hydrogenated polybutadiene (2 wt % 1.3 MDa in 15 KDa matrix) unloaded from the shear device after shear-induced crystallization (SIC) ($\Omega = 6.67$ rad/s for $t_s = 20$ s at $T = 388$ K, $d = 0.5$ mm). The effects of secondary flow (caused by elastic instabilities) appearing at long shear times. The vectors labeled with letters P and A show transmission azimuth of the polarizer and the analyzer, respectively. The small vectors across the diameter (PI) show the direction of the local orientation of lamellae (SAXS, Bruker Nanostar). Every second SAXS patterns surround the image, the numbers on the patterns correspond to the sequence of the vectors and their position along the diameter. The vectors of orientation corresponding to the first and the last SAXS pattern are appropriately labeled. The scale bar shown in the top left corner pattern corresponds to 0.05 $Å^{-1}$.

sample (Figure 6c) also confirms anisotropy in the orientation parallel to the shear flow direction. Furthermore, the P_2 function changes a slope at a point where isochromatic fringes appear in the PI (indicated by green arrows in the Figure 6) suggesting that another structural morphology is produced which contributes to the orientation of the lamellae. This point, in analogy with the boundary conditions detected for the sample sheared at temperatures above T_{ms} (Figure 3), should be associated with $\dot{\gamma}_b$ of the formation of oriented shish nuclei. Thus, both the observed PI (Figure 6b) and the degree of orientation (Figure 6c) for the sample sheared at temperatures below T_{ms} could be a superposition of structural effects produced by elongated spherulites, residual strain and oriented shish kebab morphology. However, the P_2 function suggests (Figure 6c) that the side effects such as elongated spherulites and residual strain will not significantly effect the measured position of the boundary associated with the formation of shish kebab morphology. Also, the elongated spherulites morphology can be excluded from this consideration by performing SIC experiments at temperatures above T_{ms}, which enables a temperature-driven nucleation of spherulites during flow to be avoided.

The use of the torsional parallel disks geometry is not without problems of its own as there is an influence of secondary flows which can displace regions with shear-induced nuclei into the center of the sample.[3] Indeed, such a flow can be caused by elastic instabilities and has been observed in polymer melts and solutions.[39] It becomes prominent at a certain stage of shearing when high strain has been applied to a sample and could certainly occur at the high shear rates and strain applied in industrial processes. However, as has been observed herein the formation of the oriented morphology requires moderate shear rate and strain. If secondary flow would be significant and affect the boundary conditions then the results would not be reproducible with different shear flows (Figure 4 and 5).

One advantage of postcrystallization characterization of sheared samples using polarized light imaging is that the appearance of secondary flow can be revealed. The existence of a relatively sharp boundary between the oriented and unoriented parts of polarized light images means that it is an effective approach for measurements of critical flow parameters. After a certain number of shear units the effect of secondary flow becomes noticeable and destroys the whole boundary with elastic instabilities dominating the flow. This phenomena can be clearly observed in PIs of sheared HPBD blends as a spiral superstructure.[2] A similar effect can be found in propylene−ethylene random copolymer used in this work (Figure 7), where samples after SIC with an increasing levels of strain (controlled by a shear pulse duration) reveal no orientated morphology for a short shear pulse (Figure 7a), an appearance of the boundary indicating oriented morphology at a longer shear pulse (Figure 7b), which progresses toward the center of the sample at more shear (Figure 7c), and finally, disappearance of the boundary with undulating features resembling a few overlapped spirals covering the whole sample (Figure 7d). A coexistence of a clear boundary for shear-induced nucleation toward the center of the sample with some signs of the undulations caused by secondary flows toward the edge observed in Figure 7c indicates flow conditions where the elastic instabilities kick in. Since the methodology proposed in this study enables the effect of a secondary flow to be identified, it is possible to avoid this effect by setting shear flow parameters just above the parameters required for the formation of shish nuclei (oriented morphology) and far from the conditions where the secondary flow becomes dominant.

The characteristic features of secondary flow have not been observed for LDPE. The samples have rather been destroyed before the formation of any noticeable undulations (Figure 5a). This result could be expected in a view of the previous discussion. The polydispersity of the LDPE used in this study, is much higher than HPBD and PP (see Appendix). Polymers with narrow molecular weight distribution (MWD) are known to show melt-flow instabilities more easily than their broad MWD counterparts.[39] This stabilization effect is attributed to the wider distribution of relaxation times and processes present in the broadly distributed material which damp the flow instabilities as polydispersity, M_w/M_n, increases.

In order to further analyze the structure induced by flow instabilities the bimodal HPBD blend was studied by SAXS. This blend is composed of polymers with narrow MWD (see Appendix) and should demonstrate pronounced elastic instabilities. Conditions of shearing were found where a pattern of a spiral flow just appears in the sample after SIC (Figure 8). A SAXS scan across the diameter of the sample after SIC show

orientation of the lamellar structure in a good correlation with the directions of the flow observed in the polarized light images of the sample. The orientation seen in the SAXS patterns makes a 180 deg rotation at the center of the sample perpendicular to the orientation registered at the edge of the sample. As a result of elastic instabilities, which are still not well understood and therefore difficult to control, different angles of lamellae orientation can be detected in the polymer after SIC.

In the majority of online experiments on shear-induced crystallization using torsional parallel disks geometry the X-ray patterns are taken from a single point in the disk which for a given angular speed defines the shear rate of interest.[19,25,40,41] The relationship of the shear-induced nuclei to the flow mean that these single point measurements should show the lamellae normals to be oriented with the flow as shown in Figures 3 and 6. In many online SAXS measurements of shear-induced crystallization [19,25,40,41] the orientation of the lamellae structure is shown to be tilted with respect to the flow direction and this is most likely a result of a spiral flow caused by elastic instabilities. A particularly good example of this phenomenon is shown in Figures 8 and 9 of ref 40, and it has been subsequently demonstrated that the materials therein were particularly susceptible to elastic instabilities due to their combination of narrow molecular weight distributions and long relaxation time. An advantage of post-crystallization characterization of the radial distribution of orientation of the lamellar, compared with detecting at a single point as in the online experiments, is that this effect of elastic instability can be identified.

It is well-known fact that elastic instabilities may occur in a shear flow of viscous highly elastic fluids. In flows with rotational geometry this effect is caused by stretched polymer molecules leading to a radial pressure gradient. Similar effect can be found in inertial flows with a pressure drop driven by centrifugal forces. It has been recently found that the analogy between inertial and elastic secondary flows extends further; for example, at high enough Weissenberg number ($W_i \sim 10$) elastic parallel disk flows can show a highly irregular state with spatial and temporal characteristics similar to those of turbulence[42] with the sequence of bifurcations in a viscoelastic fluid that transforms simple shearing flow to 'elastic turbulence'.[43] This phenomenon has been identified in model dilute solutions of high molecular weight polymers using coloring particles to visualize the flow behavior. Analogous effects can be found in typical polymers crystallized under shear (Figure 7 and 8) where the complex oriented structure caused by elastic instabilities is pinned by the process of crystallization and persists down to room temperature. SAXS and PI measurements from samples with a high strain (and hence a large W_i) show that the orientation of the lamellae can have a very complicated structure produced by a spiral flow similar to the patterns caused by elastic turbulence.[42,43]

After SIC in torsional parallel disks geometry, well chosen materials and flow conditions show a clear boundary between oriented and unoriented regions by all the analytical methods used for structural characterization herein (Figure 3, follow the blue arrows given for guidance). The macrostructure of the samples can be represented as a slice of a big spherulite with the core removed. The combinatorial approach proposed to measure the critical parameters required for the onset of oriented morphology, covers the range of shear rates from zero up to a maximum value controlled by the radius of the sample and the angular speed of the rotating disk (eq 1). The higher the angular speed is the higher the maximum value of the shear rate experienced by the polymer. In this case if the range of shear rates used in the experiment covers the onset of orientation, then a boundary between the oriented and unoriented parts should appear and move toward the center of the sample with longer shear pulses. This effect can be visually observed on

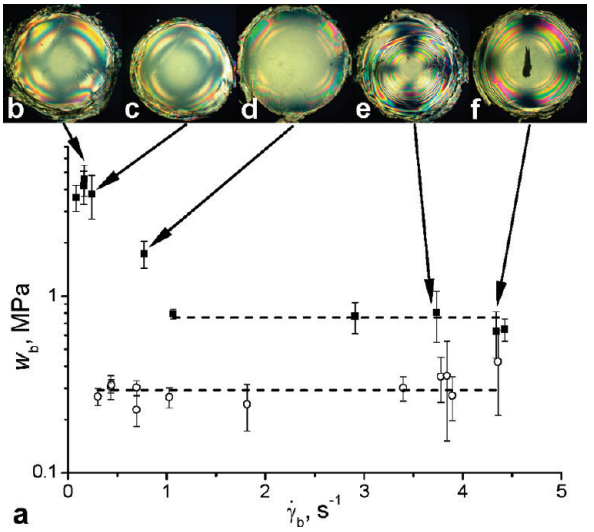

Figure 9. (a) Plot of the boundary specific work, w_b, versus the boundary shear rates, $\dot{\gamma}_b$, representing the boundary conditions required for the formation of oriented nuclei in the sheared low density polyethylene (Lupolen 1840H) measured at temperatures above the melting point of spherulites (T = 385 K, solid squares) and below (T = 377 K, open circles). The dashed lines represent the line of the critical specific work, w_c, obtained by a linear fitting with a zero slope to the flatten zone of the graphs ($w_c = 0.75 \pm 0.03$ MPa, T = 385 K; $w_c = 0.29 \pm 0.01$ MPa, T = 377 K). (b−f) Representative polarized light images of the sheared samples used for the measurements of the boundary conditions [(b) Ω = 0.017 rad/s for t_s = 3000 s at T = 385 K; (c) Ω = 0.033 rad/s for t_s = 1440 s at T = 385 K; (d) Ω = 0.067 rad/s for t_s = 120 s at T = 385 K; (e) Ω = 1.07 rad/s for t_s = 6 s at T = 385 K; (f) Ω = 0.53 rad/s for t_s = 4 s at T = 385 K]. The width of the polarized light images is equivalent to 18 mm. Note the logarithmic scale of the specific work axis.

LDPE samples where opaque area corresponds to spherulitic unoriented structure and the transparent area to oriented structure (Figure 5).

Measurements of Critical Flow Parameters for the Formation of an Oriented Morphology

Polyolefins with a wide polydispersity as well as model polyolefin blends of narrow polydispersity demonstrate a clear boundary between oriented and unoriented regions under flow. Results on measurements of the critical flow parameters required for the formation of oriented nuclei in shear-induced crystallization of bimodal blends of hydrogenated polybutadiene have been previously reported.[2] The new results presented in this paper will be restricted to polydisperse industrial polymers. These polymers produce similar effects in lamellar orientation to the model bimodal HPBD blends, but due to the continuous distribution in molecular weights, and hence relaxation times, the behavior of the critical flow parameters can be more complicated.

Low-Density Polyethylene (LDPE). The boundary conditions measured from a set of LDPE samples sheared for different times at different angular speeds at temperature above the melting point of LDPE spherulites, T_{ms} = 385 K, demonstrate a dependence of w_b versus $\dot{\gamma}_b$ (Figure 9a) similar to that observed for HPBD bimodal blends.[2] The data clearly demonstrate that the boundary specific work is constant within a wide range of boundary shear rates. Thus, the criterion of specific work appears to be equally valid for the industrial polymer as it was for the model bimodal blends. In the model blends there was a sharp increase of the specific work at small boundary shear rates associated with the singular Rouse time of the longest molecules whereas there is a continuous increase of critical specific

work at shear rates below 1 s^{-1} for the LDPE. If this parameter, $\dot{\gamma}_{min}^{LDPE,385\ K}$, could be associated with the Rouse time of the most slowly relaxing molecules present in the polymer ensemble, in analogy with the model HPBD blends[2], then their relaxation time would be about 1 s. Even if this estimate is not absolutely correct (as it is difficult to model relaxation processes for branched molecules like LDPE and the Rouse time should be properly associated with a particular molecule and not to be an averaged value describing a polydisperse system), the relaxation time observed suggests that a very long time is required for the LDPE molecules to relax after stretching during shear. This value is of the same order of magnitude as the Rouse time reported for other branched polyolefins.[40] LDPE has a broad and continuous MWD with some chains bigger than 2 MDa. The absence of clearly defined cutoff in the boundary specific work at low shear rates, unlike the model blends, suggests that this effect is related to polydispersity of the sample: there will always be some polymers long enough to initiate shish nuclei even at vanishing small shear rates. Higher shear rates stretch shorter molecules and, therefore, increase the concentration of stretched molecules which can be potentially involved in the formation of shish nuclei.

The measurements of the boundary parameters for the polymer sheared at temperature below the melting point of the LDPE spherulites, $T = 377$ K, show constant value of the boundary specific work within the range of the measured boundary shear rates (Figure 9a). This observation suggests that the minimum shear rate, $\dot{\gamma}_{min}^{LDPE,377\ K}$, should be below the values accessible with the experiments performed herein. A reduction of the angular speed to resolve measurements of the boundary specific work at lower shear rates requires a significant increase of the shearing time to achieve the necessary boundary specific work. Consequently, the increase in shearing time at temperatures below T_{ms} increases the number of spherulitic nuclei formed in the material during the long shear pulse, these may be more numerous than the shish nuclei formed by the weak flow and dominate the crystallization process. The amount of the material crystallized in the oriented shish kebab morphology will be scarce and is unlikely to be detected in the experiment.

These results suggest that the formation of the oriented shish nuclei in the LDPE melt occurs at very moderate conditions (Figure 9). A shear pulse at a rate of few reciprocal seconds for few seconds is actually enough to create the orientation. These flows are far weaker than those experienced in industrial processes exploring hundreds of reciprocal seconds for injection molding.[44]

LDPE exhibits shear thinning over a wide range of shear rates and the viscosity can be approximated as a power law

$$\eta(\dot{\gamma}) = k \cdot \dot{\gamma}^{n-1} \tag{4}$$

where k is the polymer-related constant and n is the power-law index.[20,45] Taking the simplified definition of the specific work (eq 3) and the fact that the boundary specific work is constant at shear rates $\dot{\gamma}_b > \dot{\gamma}_{min}$, the boundary shear rate required for the orientation, $\dot{\gamma}_b$, should have a power law dependence on time of shearing:

$$\dot{\gamma}_b(t_s) = \left(\frac{w_c}{k \cdot t_s}\right)^{1/n+1} \tag{5}$$

Since shear thinning of the LDPE is already observed at 0.003 rad/s and it has a fully developed power law regime above 0.01 rad/s, which is much less than the shear rates of interest $\dot{\gamma}_b > 1$ rad/s where the boundary specific work is constant, then the viscosity can be considered as a power-law of the shear rate (eq 4) and the expression for the boundary shear rate (eq 5) should be valid. Thus, at shear rates above $\dot{\gamma}_{min}$ the boundary shear rate required for the formation of oriented shish nuclei will decrease following a power law dependence on increase of time of shearing, t_s. A fit of the $\dot{\gamma}_b$ data (Figure 10b) within the range of shear rates $\dot{\gamma}_b > \dot{\gamma}_{min}$ using eq 5 should produce the same n parameter as the power law viscosity equation (eq 4) applied to the viscosity data measured from rheology (Figure 10a). Thus, viscosity of the polymer, in particular its shear-thinning, can be estimated from shear-induced crystallization of polymer. Indeed, there is a good correlation between n parameters obtained from boundary conditions for the formation of oriented nuclei during SIC and from viscosity of the polymer measured by rheology (Table 1). This comparison suggests that the viscosity of the polymer as a measure of resistance of the polymer to the flow is one of the factors controlling both the molecules behavior in the polymer melt and the formation of oriented nuclei. It should be noted, however, that the high shear rate region will require a short shearing time which can become comparable with a time scale of the nonlinear response of the polymer upon a ballistic shear pulse. This effect cannot be neglected and the boundary shear

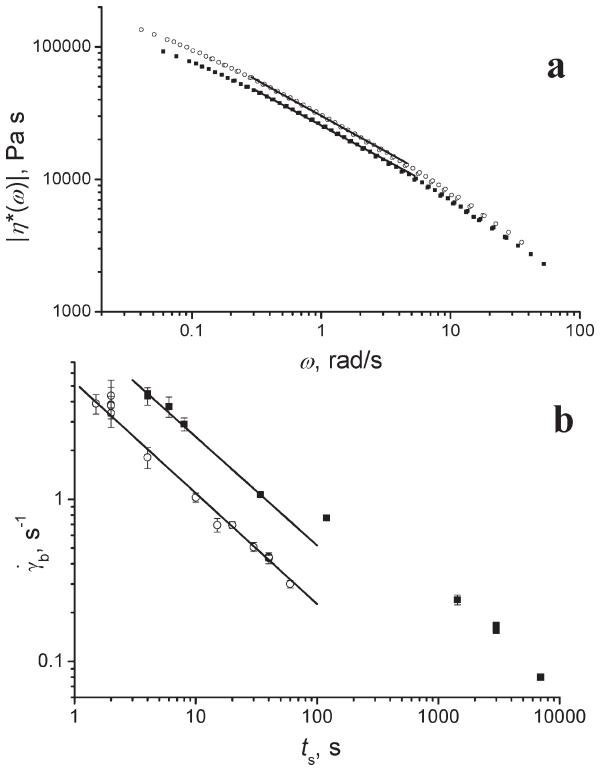

Figure 10. (a) Modulus of complex viscosity of LDPE (Lupolen 1840H), obtained from a master curve of frequency sweep rheology measurements by a shift to $T = 377$ K (open circles) and $T = 385$ K (solid squares), fitted within the chosen range of angular frequency, ω, with the power law model $\eta(\dot{\gamma}) = k \cdot \dot{\gamma}^{n_v-1}$ assuming the Cox−Mertz rule $\eta(\dot{\gamma}) = |\eta^*(\omega)|$ for $\omega = \dot{\gamma}$ (solid lines). The viscosity parameter, n_v, is presented in Table 1. (b) Plot of the boundary shear rates, $\dot{\gamma}_b$, versus time of shearing, t_s, required for the formation of oriented nuclei, measured at temperatures above the melting point of spherulites ($T = 385$ K, solid squares) and below ($T = 377$ K, open circles). The points of the graphs fitted with the function $\dot{\gamma}_b(t_s) = (w_c/kt_s)^{1/(n_b+1)}$ (solid lines), where w_c is the critical specific work of the polymer corresponding to the flatten area of the boundary specific work presented in the Figure 9. The boundary shear rate parameter, n_b, is presented in Table 1.

Table 1. Comparison of the Power Law Parameter, *n*, Obtained either from the Fitting of the Viscosity Data (Figure 10a or 13a) or the Boundary Shear Rate Measurements (Figure 10b or 13b) of LDPE (Lupolen 1840H) or Propylene−Ethylene Random Copolymer, Respectively, at Different Temperatures

polymer	*T*, K	viscosity parameter, n_v	boundary shear rate parameter, n_b
LDPE	385	0.476 ± 0.004	0.49 ± 0.03
	377	0.460 ± 0.004	0.46 ± 0.04
propylene−ethylene random copolymer	443	0.375 ± 0.005	0.39 ± 0.05
	438	0.373 ± 0.006	0.45 ± 0.14
	413	0.349 ± 0.005	0.40 ± 0.19

rate will not follow the power law line (eq 5 and Figure 10b) under such conditions.

So far only boundary parameters, easily accessible for LDPE from PI measurements, have been taken into consideration for the formation of oriented shish nuclei. It can be assumed that the amount of work supplied to the polymer by shear flow above the boundary conditions should control the number of oriented nuclei formed. This number should be proportional to the work applied to the polymer and if the specific work is the only parameter responsible for the formation (and stabilization) of the oriented nuclei at $\dot{\gamma}_b > \dot{\gamma}_{min}$, then the shear conditions, controlled by both the angular speed and the shearing time, should be described through the specific work parameter. SAXS measurements of the degree of orientation (P_2), used to detect boundary conditions for the formation of oriented structure along with PI measurements, should also contain quantitative information about the number of oriented nuclei formed. Every radial point of the sample associated with a particular shear rate is also associated with a certain amount of work applied to the polymer during shear. The specific work experienced by the polymer during shear, *w*, can be calculated for each point in accordance with eq 2 replacing $\dot{\gamma}_b(t)$ by $\dot{\gamma}(t)$ obtained from radial distribution of shear rates across the sample. The degree of orientation, obtained from a SAXS scan, plotted versus *w* shows that the degree of orientation of the samples corresponding to the region of the constant boundary specific work, associated with w_c, essentially collapses onto a master curve (Figure 11a). All the samples show an increase of the degree of orientation above w_c and no orientation in a zone where the polymer experienced $w < w_c$. Some drop in the measured degree of orientation at $w \sim 2.5$ MPa (Figure 11a) is caused by elasticity of the LDPE polymer (Figure 6). The point in the curve where the degree of orientation becomes nonzero, obtained for a particular sample, corresponds to the point associated with the same sample on the boundary specific work curve measured from PI (Figure 9a). Consistent with the PI measurements (Figure 9a) the sample with the boundary associated with the shear rates below $\dot{\gamma}_{min}^{LDPE,385\ K}$ (Figure 11a, $\Omega = 0.033$ rad/s and $t_s = 1440$ s) demonstrates an increase of orientation at the specific work values higher than w_c. In analogy with the samples sheared at temperature above melting point of LDPE spherulites (Figure 11a), the degree of orientation versus the specific work forms a master curve (Figure 11b) for all the samples sheared at temperatures below the melting point of LDPE spherulites. Since these samples have their boundaries associated with the same value of specific work (Figure 9a), this is an expected result. However, in contrast to the results obtained for the samples sheared at $T > T_{ms}$ (Figure 11a), the degree of orientation measured for the samples sheared at $T < T_{ms}$ is nonzero with a slight increase in the region of the specific work values below

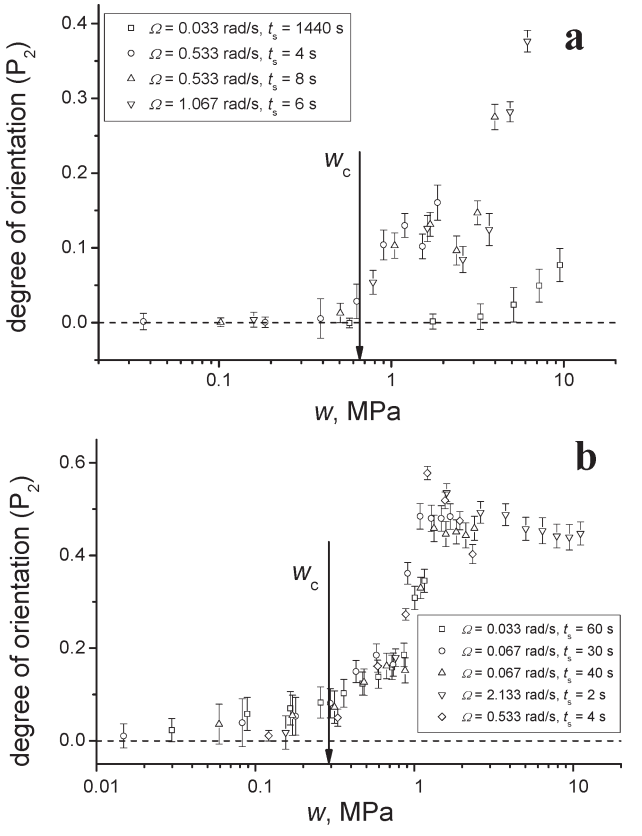

Figure 11. Combined plots of degree of orientation of the lamellar structure of LDPE (Lupolen 1840H), calculated from radial SAXS scans of the sheared samples, versus specific work experienced by the polymer during the shear pulse at $T = 385$ K (a) and $T = 377$ K (b). The corresponding shear pulse parameters are presented on the plots. The specific work values have been calculated from the radial distribution of shear rates by integration $w(r) = \int_0^{t_s} \eta[\dot{\gamma}(r,t)]\dot{\gamma}^2(r,t)\,dt$, where $\dot{\gamma}(r,t) = \Omega(t) \times r/d$ and $d = 0.5$ mm is the thickness of the gap between the shearing disks. The value of the critical specific work, w_c, measured from the polarized light images (Figure 9), is indicated by the arrows. Dotted lines corresponding to zero degree of orientation are shown. Note the logarithmic scale of the specific work axis.

w_c (Figure 11b). This effect, as discussed before (Figure 6), is caused by the fact that the measured degree of orientation is a product of two orientations originating from elongated spherulites, which are noticeable as a nonzero P_2 function at $w < w_c$, and shish nuclei forming at $w > w_c$ which dominate this region. There is saturation in the degree of orientation at $w > 1$ MPa which could be a result of either saturation of number of oriented nuclei created at these conditions or crystal growth-related process.

Propylene−Ethylene Random Copolymer (PP). A propylene−ethylene random copolymer (see Appendix) produced similar behavior in the boundary condition parameters measured at different time and shear rates (Figure 12) to LDPE (Figure 9). There is a wide range of shear rates where the boundary specific work is constant with a continuous increase of orientation in the region of small shear rates. In analogy with LDPE data (Figure 9a) the increase of the boundary specific work measured for the polymer sheared at temperatures below the melting point of PP spherulites is less distinctive than the cutoff observed for the model HPBD blends.[2] The representative set of data obtained for the PP sheared at 438 K clearly shows that the increase of the specific work required for the formation of oriented nuclei at this temperature is observed at boundary shear rates below $\dot{\gamma}_{min}^{PP,438\ K} = 100\ s^{-1}$ (Figure 12a). This suggests that molecules

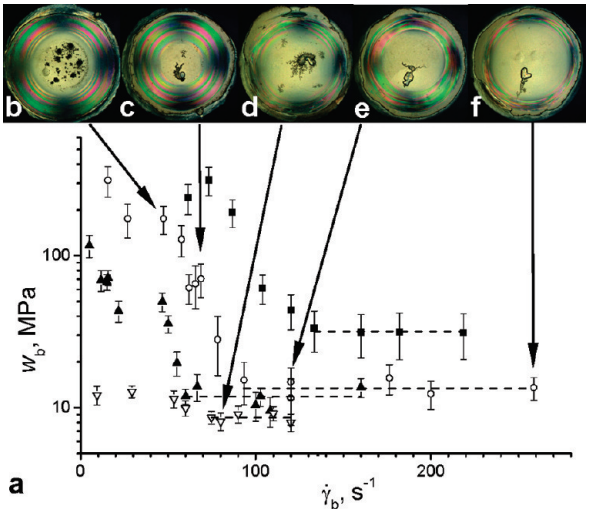

Figure 12. (a) Plot of the boundary specific work, w_b, versus the boundary shear rates, $\dot{\gamma}_b$, representing the boundary conditions required for the formation of oriented nuclei in the sheared propylene−ethylene random copolymer measured at temperatures above the melting point of spherulites (T = 443 K, solid squares; T = 438 K, open circles; T = 433 K, solid triangles up) and below (T = 413 K, open triangles down). The dashed lines represents the critical specific work, w_c, obtained by a linear fitting with a zero slope to the flatten zone of the graphs (w_c = 31.7 ± 0.5 MPa, T = 443 K; w_c = 13.4 ± 0.6 MPa, T = 438 K; w_c = 11.8 ± 0.7 MPa, T = 433 K; w_c = 8.6 ± 0.2 MPa, T = 413 K,). (b−f) Representative polarized light images of the sheared samples used for the measurements of the boundary conditions [(b) Ω = 5 rad/s for t_s = 80 s at T = 438 K; (c) Ω = 10 rad/s for t_s = 20 s at T = 438 K; (d) Ω = 10 rad/s for t_s = 1.33 s at T = 413 K; (e) Ω = 13.3 rad/s for t_s = 2 s at T = 438 K; (f) Ω = 20 rad/s for t_s = 0.67 s at T = 438 K]. The width of the polarized light images is equivalent to 18 mm. Note the logarithmic scale of the specific work axis.

with a Rouse time of 0.01 s ($1/\dot{\gamma}_{min}^{PP,438\ K}$) or above in the copolymer ensemble are mostly likely responsible for the formation of oriented nuclei. Rheological measurements of this polymer at 438 K give a plateau modulus $G_N^0 \sim 0.1$ MPa and the entanglement molecular weight is estimated to be $M_e \sim 36$ kDa. This value, together with the reptation time τ_d = 0.06 s (estimated from the crossover of storage and loss moduli, G' and G'') and molecular weight of the polymer M_w = 252 kDa can be used to estimate the Rouse time of the copolymer molecules $\tau_R = \tau_d M_e/(3M_w) = 0.003$ s and, therefore, the shear rate required for the molecules to be in a stretched state to create oriented nuclei is given by $\dot{\gamma} > 1/\tau_R \sim 300\ s^{-1}$. Even though these estimates are not absolutely accurate, due to polydispersity, the estimated value of the shear rate required for the formation of oriented nuclei is of the same order of magnitude as the value obtained from the experimental plot of the boundary specific work (Figure 12a), suggesting that the stretching of the molecules is the necessary condition for the formation of oriented nuclei. The significant difference in this parameter with the shear rates observed for the LDPE ($\dot{\gamma}_{min}^{PP,438\ K} = 100\ s^{-1}$ versus $\dot{\gamma}_{min}^{LDPE,385\ K} = 1\ s^{-1}$), suggesting that the LDPE relaxes much slower than the PP, should be associated with the temperature, the molecular weight, and the architecture of the molecules. Indeed, the first two parameters would contribute into the decrease of the relaxation time since both an increase of the temperature and a decrease in the molecular weight of the high molecular weight tail would result in a reduction in the relaxation time and thus an increase the minimum shear rate parameter (which is inversely proportional to the relaxation time). The increase of the boundary specific work with temperature,

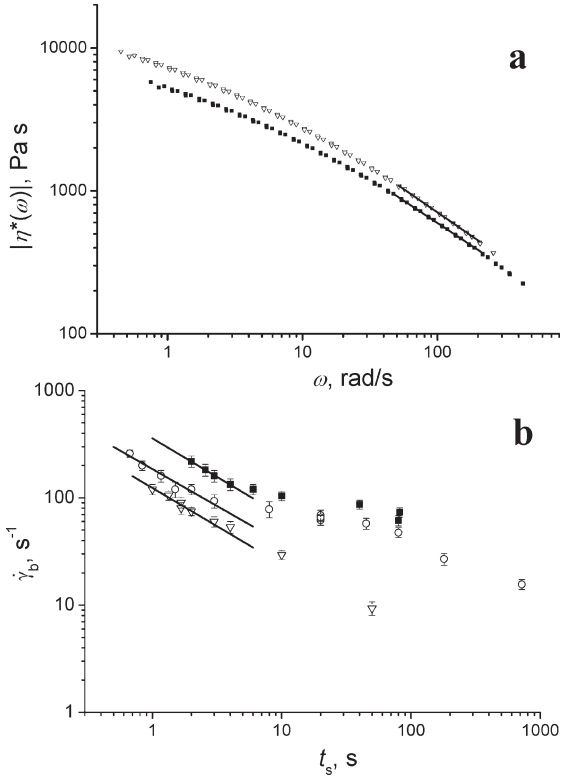

Figure 13. (a) Modulus of complex viscosities of the propylene−ethylene random copolymer (PP), obtained from master curve of frequency sweep rheology measurements by a shift to T = 413 K (open triangles down) and T = 443 K (solid squares), fitted within the chosen range of angular frequency, ω, with the power law model $\eta(\dot{\gamma}) = k\cdot\dot{\gamma}^{n_v-1}$ assuming the Cox−Mertz rule $\eta(\dot{\gamma}) = |\eta^*(\omega)|$ for $\omega = \dot{\gamma}$ (solid lines). The viscosity parameter, n_v, is presented in Table 1. (b) Plot of the boundary shear rates, $\dot{\gamma}_b$, versus time of shearing, t_s, representing the flow conditions required for the formation of oriented nuclei in the sheared PP measured at temperatures above the melting point of spherulites (T = 443 K, solid squares; T = 438 K, open circles) and below (T = 413 K, open triangles down). The points of the graphs fitted with the function $\dot{\gamma}_b(t_s) = (w_c/kt_s)^{1/(n_b+1)}$ (solid lines), where w_c is the critical specific work of the polymer corresponding to the flatten area of the boundary specific work presented in Figure 12. The boundary shear rate parameter, n_b, is presented in Table 1.

observed in PP (Figure 12a) once more indicates its temperature dependence, pointing toward the fact that thermal vibrations of the molecules are one of controlling factors of shish nuclei formation. These data also show that oriented shish nuclei, created by flow, are quite stable and shearing at temperatures 16 K above the melting of PP spherulites still produces an oriented structure where a spherulitic morphology is unlikely to be formed. These data confirm previous conclusions concerning the stability of thread-like precursors made on the S, T-diagram for polypropylene.[28]

Following the previous discussion on the viscosity of the LDPE (Figure 10) plotting of the PP data produces similar results (Figure 13). There is a good correlation between power law parameter in the viscosity equation, n, obtained from both rheology data (Figure 13a) and the boundary conditions for the formation of oriented morphology measured from samples after SIC (Table 1).

The plot of the specific work versus degree of orientation from SAXS shows behavior similar to LDPE. There is no orientation at low values of the specific work with a threshold at the critical specific work, where the degree of orientation starts to increase with the amount of work supplied to the polymer system by shear (see Figure 14a for samples sheared above the melting point of PP spherulites,

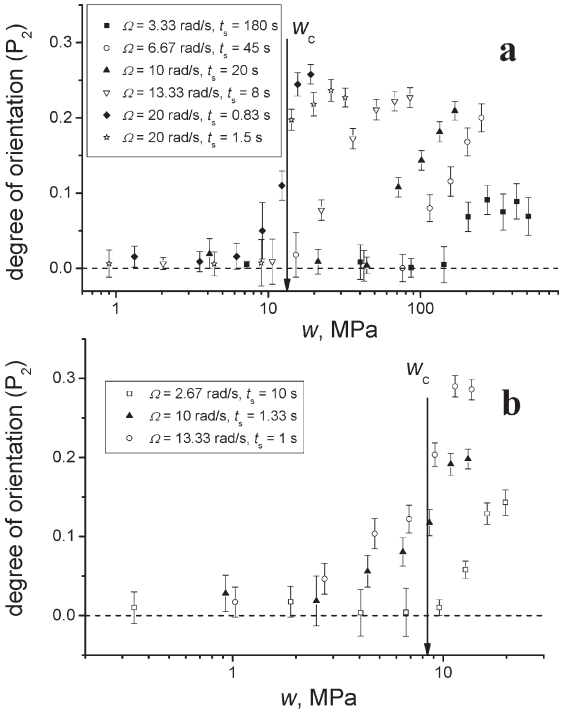

Figure 14. Combined plots of degree of orientation of the lamellar structure of the propylene−ethylene random copolymer, calculated from radial SAXS scans of the sheared samples, versus specific work experienced by the polymer during the shear pulse at $T = 438$ K (a) and $T = 413$ K (b). The corresponding shear pulse parameters are presented on the plots. The specific work values have been calculated from the radial distribution of shear rates by integration $w(r) = \int_0^{t_s} \eta[\dot{\gamma}(r,t)]\dot{\gamma}^2(r,t)\,dt$, where $\dot{\gamma}(r,t) = \Omega(t) \cdot r/d$ and $d = 0.5$ mm is the thickness of the gap between the shearing disks. The value of the critical specific work, w_c, measured from the polarized light images (Figure 12), is indicated by the arrows. Dotted lines corresponding to zero degree of orientation are shown. Note the logarithmic scale of the specific work axis.

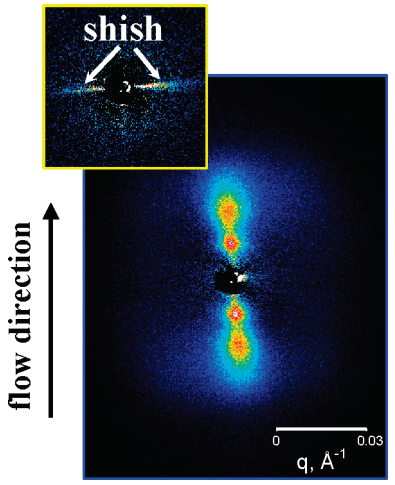

Figure 15. SAXS patterns (Diamond Light Source, station I22) of a propylene−ethylene random copolymer (PP) acquired at room temperature after shear-induced crystallization ($\Omega = 10$ rad/s for $t_s = 11$ s at temperature 433 K, the patterns have been collected at a point $\dot{\gamma} = 150$ s^{-1} corresponding to $w = 112$ MPa). The inset shows X-ray scattering of the PP collected at 433 K straight after the shear pulse. The images both have the same q-scale and the same false color intensity scale.

$T > T_{ms} = 427$ K). The samples sheared at conditions corresponding to the area where w_b is constant ($w_b = w_c$) have a degree of orientation graph following the same master curve (Figure 14a, the solid diamonds and the open stars). For the samples sheared at flow conditions producing a boundary at $\dot{\gamma}_b > \dot{\gamma}_{min}^{PP,438\ K}$, where the concentration of the stretched molecules in the melt at such shear conditions reduces, the threshold of the specific work required for the formation of oriented morphology shifts toward larger specific work values, following the trend of the boundary specific work obtained from PI measurements (Figure 12a). The results of the degree of orientation of the samples sheared at temperatures below melting point of the PP spherulites ($T = 413$ K) produces a more complicated picture caused by a simultaneous formation of elongated spherulites and shish nuclei at this temperature (Figure 14b).

The data suggest that at shear rates above $\dot{\gamma}_{min}$ the degree of orientation depends on the amount of specific work supplied to the polymer during shear, which is termed the critical specific work, w_c. This parameter unites two flow parameters such as shear time and a shear rate and if w_c is known then a set of flow parameters required for the formation of oriented structure during shear can be derived from eq 2. The degree of orientation of the polymer structure created after shear-induced crystallization is proportional to the work applied to the polymer (in the region $w > w_c$), which controls the number of oriented nuclei created and stabilized during the shear flow.

The calculated boundary specific work obtained from shear-induced crystallization experiments run at different angular speeds and duration of shearing can be plotted versus boundary shear rates and both the critical specific work, w_c, and the minimum shear rate, $\dot{\gamma}_{min}$, can be evaluated. The parameters obtained can be used to estimate the dependence of the formation of the oriented structure on both the molecular weight distribution of the polymer and the thermal conditions applied to the polymer. Subsequently, these estimates can be used to choose processing parameters for the polymer melt in industrial applications.

The formation of shish can be directly observed in a flow-induced crystallization by online SAXS measurements using a Linkam shear device fitted with Kapton film windows.[25,26,40] Following the data on boundary specific work describing the transition between oriented and unoriented morphology (Figure 12a) the flow parameters required for the formation of oriented shish kebab structure can be chosen. For example, a shear pulse of shear rate $\dot{\gamma} = 150$ s^{-1} at 433 K would require performing $w > 11.8$ MPa (w_c at 433 K, Figure 12a) to initiate the formation of shish nuclei in SIC. Since the scattering power of the particles is proportional to the square of their volume, the concentration of shishes created by flow should be high enough to be detected by online SAXS measurements. Thus, the amount of mechanical work supplied to the polymer by shear flow, controlling the number of shish nuclei formed (Figure 14), has to be significantly more then the threshold value (w_c). An order of magnitude higher work value has been used to carry out online SAXS measurements of the shish formation (Figure 15). The postshear SAXS pattern (Figure 15, inset) shows a clear meridional streak corresponding to long thin structures in the flow direction (shishes) whereas the fully crystallized pattern (Figure 15) shows scattering dominated by the two orders of reflection arising from lamellar stacks (kebabs) with the layer normal parallel to the flow. Similar patterns have been reported previously for different polymers.[22,24] The post shear pattern arising from the shish is of a much lower intensity than the reflections from the fully crystallized lamellar; however, shish structure has been resolve due to the high concentration of oriented nuclei created by a high amount of work supplied to the polymer. The tilt observed in this data is a result of elastic instabilities kicking in at higher work values after the

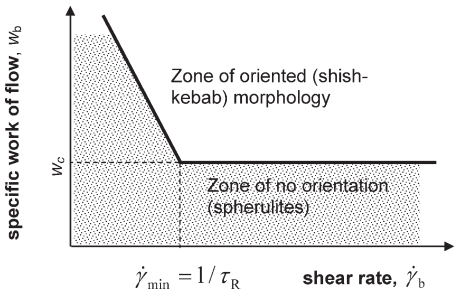

Figure 16. Schematic diagram of flow conditions required for the formation of oriented (shish kebab) morphology in a polymer melt. The solid line dividing the diagram into two zones (zone of orientation and zone of no orientation) corresponds to a plot of the boundary specific work required for the formation of oriented nuclei (shish), w_b, as a function of the boundary shear flow rate, $\dot{\gamma}_b$. The critical specific work, w_c, indicates the minimum amount of the specific work required for the formation of oriented nuclei at the chosen thermodynamic parameters. The minimum shear rate $\dot{\gamma}_{min}$ indicates the flow rate below which the concentration of molecules in a stretched state is decreased.

formation of shish nuclei (Figure 7). Even though the online experiment on shish kebab formation shows a reasonable correlation with off-line measurements the SAXS patterns are presented for the sake of demonstration only. Unfortunately, an artifact of the use of Kapton windows in the Linkam shear device for SAXS measurements does not allow systematic measurements to be made and the flow parameters reported for the presented online experiment may not be absolutely correct. In this commonly used experimental configuration steel disks with a pair of holes are covered with a thin membrane (Kapton film) to allow X-ray transmission. The flexibility of the films results in their bulging due to the normal force created by the polymer experienced flow and this introduces changes in the gap between flexible parts of the disks during the shear pulse. Thus, gap deviations, which are out of control in this setup, can be a source of systematic errors especially at high shear rates and long pulse duration.

Conclusions

The findings can be concisely described as follows. Oriented structures only form if the polymer has experienced more than a certain amount of work performed on its melt at shear rates, $\dot{\gamma}$, above rates inversely proportional to Rouse time, τ_R, of the longest chains in the polymer ensemble ($\dot{\gamma} > 1/\tau_R$). Chains with a longer relaxation time in the polymer ensemble have to be stretched by shear flow to be able to form shish nuclei upon which the bulk of the material could crystallize as kebabs. A schematic diagram of the flow parameters required for the formation of oriented shish kebab morphology, based on a plot of the specific work required for the formation of oriented nuclei, w_b, versus shear rates, can be suggested (Figure 16). The diagram shows that w_b is constant over a wide range of shear rates and can be thus used as a critical parameter, w_c, to signify the formation of shish kebab structure. For polydisperse materials there is an increase in this parameter below a certain shear rate, $\dot{\gamma}_{min}$. This shear rate is associated with Rouse time, $\dot{\gamma}_{min} = 1/\tau_R$, characterizing the population of molecules in the polymer responsible for the formation of oriented nuclei. Since only longer molecules, characterized by longer relaxation time, can be stretched at lower shear rates and involved in the initial stage of oriented nuclei formation the increase of the specific work at shear rates below $\dot{\gamma}_{min}$ is associated with molecular weight distribution of the polymer. The magnitude of the specific work required to create shish kebab structures depends on both the chemical structure of the polymer and its molecular weight distribution as these both affect the longest relaxation time.

A method which can be used to measure critical parameters for the onset of orientation in semicrystalline polymers has been developed and its application to a range of industrial materials is shown. Where the sample is transparent polarized light imaging can be used exclusively to make the measurements whereas if the material is opaque (due to multiple scattering of visible light) X-ray (and/or neutron) scattering measurements of the orientation must be applied.

Acknowledgment. The autors are garetful to EPSRC for support (Grants GR/T11852/01 and GR/T11807/01) and to the μPP consortium (http://www.irc.leeds.ac.uk/mupp/), especially Christine Fernyhough and Choon Chai for the supply of materials and Peter Olmsted, Richard Graham, Alexei Likhtman and Tom McLeish for lengthy discussions.

Appendix: Materials, Instruments and Data Analysis

Three different polymer materials were used to demonstrate the method of measuring the critical parameters of shear flow required for the formation of oriented nuclei (1) a commercial low density polyethylene (LDPE, Lupolen 1840H, Basell, M_n = 17 kDa, M_w = 240 kDa, polydispersity $M_w/M_n \sim 14$, T_{ms} = 385 K), (2) a propylene−ethylene random copolymer [PP, Ineos, M_n = 34 kDa, M_w = 252 kDa, $M_w/M_n \sim 6$, with ethylene fraction of 3.6 wt % estimated from the peak melting point of the polymer (T_{pms} = 418 K),[46] T_{ms} = 427 K], and (3) a model blend of hydrogenated polybutadiene composed of laboratory synthesised polymers[47] with a narrow distribution of molecular weights (HPBD, 2 wt % 1.3 MDa in 15 kDa matrix with M_n = 950 kDa, M_w = 1.33 MDa, $M_w/M_n \sim 1.4$ and M_n = 14 kDa, M_w = 15 kDa, $M_w/M_n \sim 1.1$, respectively, and T_{ms} = 386 K). While the results on the first two materials, characterized by high polydispersity, are described in detail to justify the methodology the results on the model HPBD blends of controlled polydispersity, reported previously,[2] are mainly invoked in the sections dedicated to understanding the phenomena observed in shear-induced crystallization.

To prepare samples for shear-induced crystallization experiments polymers (powder or granules) have been kept in a vacuum oven at temperatures above the melting point of spherulitic morphology of the polymers to remove air bubbles, then cooled down and transferred to a hot press to make films of required thickness (0.05 mm more then the gap used in the shear experiments). Disks are mechanically punched from the films prior to loading in the shear device. A modified Linkam shear device (CSS 450) has been used to carry out experiments on shear-induced crystallization. The modifications of this device are discussed in details in the section dedicated to shear instruments.

In accordance with the shear-temperature protocol (Figure 1) the following temperature parameters have been used in this study for SIC: LDPE [I, the samples heated up from room temperature to 443 K at a rate of 0.5 K/s kept at this temperature for 600 s and cooled down to the temperature of shearing (377 or 385 K) at a rate of 0.33 K/s; II, the samples kept at the temperature of shearing for 3600 s; III, the samples cooled down to 363 K at a rate of 0.0167 K/s and then to room temperature (293 K) at a rate of 0.33 K/s and finally unloaded from the shear device] and PP [I, the samples heated up from room temperature to 493 K at a rate of 0.5 K/s kept at this temperature for 600 s and cooled down to the temperature of shearing (413 K, 433 K, 438 or 443 K) at a rate of 0.33 K/s; II, the samples kept at the temperature of shearing for 3600 s; III, the samples cooled down to 403 K at a rate of 0.0167 K/s and then cooled down to room

temperature (293 K) at a rate of 0.33 K/s and finally unloaded from the shear device].

The structural morphology of the samples unloaded from the shear device after SIC experiments has been analysed by polarized light imaging and small angle- and wide angle X-ray scattering methods (SAXS and WAXS, respectively). Since a whole image of a sample has been required to identify the boundary between oriented and unoriented part of the sample, PI has been performed by taking images of the disk using a plane polariscope setup with crossed polarizer and analyzer, white light source, and a CCD camera. SAXS measurements have been performed either at synchrotron sources (SRS Daresbury Lab, station 2.1 and Diamond Light Source, station I22 both equipped with a RAPID area detector) or using a laboratory SAXS instrument (Bruker Nanostar, Cu Kα radiation, equipped with a HiStar area detector and a semi-transparent beamstop). This information is specified in the figure captions. The SAXS measurements have been used to measure degree of orientation of lamellar structure in semi-crystalline polymers after shear-induced crystallization. Two dimensional SAXS patterns have been azimuthally integrated and the obtained intensity patterns, $I(\phi)$, have been used to calculate the Herman's orientation function (P_2) defined as:

$$P_2 = \frac{3\langle \cos^2 \phi \rangle - 1}{2} \tag{A1}$$

where

$$\langle \cos^2 \phi \rangle = \frac{\int_0^{\pi/2} I(\phi) \cos^2 \phi \sin \phi \, d\phi}{\int_0^{\pi/2} I(\phi) \sin \phi \, d\phi}$$

is the average angle that the lamellar normal makes with a chosen direction, which in this work is associated with the flow direction. It has also been assumed in the expression of the average angle that there is a uniaxial orientation with symmetry around the shear direction which enables the integration over the whole solid angle to be neglected. Since the experimental intensity data have a discrete distribution, analytical integration in the formula has been replaced by numerical integration.

WAXS patterns have been selectively recorded for oriented and unoriented parts of some sheared samples to identify crystal phase composition of the polymers and orientation of the crystals. The polymer disks unloaded after SIC were mounted on a single crystal diffractometer (Bruker X8 APEX, MoK_α radiation, equipped with an APEX II CCD detector) with the X-ray beam direction normal to the plane of the disks.

The viscosity of the samples has been measured by a rheometer with either cone−plate or plate−plate geometry (AR-G2, TA Instrument). The complex viscosity of the polymers obtained from frequency sweep rheology measurements at different temperatures have been time-temperature shifted to the temperatures at which shear pulse has been applied to the polymers in the shear-induced crystallization. The obtained data has been fitted with an empirical equation originating from the Cross model[48]

$$|\eta^*(\omega)| = \frac{\eta_1}{1 + (\omega/\omega_1)^{\alpha_1}} + \eta_2 \tag{A2}$$

where $\eta^*(\omega)$ is the linear complex viscosity, ω is a circular frequency and η_1, η_2, ω_1, and α_1 are fitting parameters. Assuming the Cox−Merz rule $\eta(\dot{\gamma}) = \eta^*(\omega)$ for $\omega = \dot{\gamma}$ the obtained parameters have been used further in the calculations of specific work. In some cases a simplified form of power law expression for viscosity has been used $\eta(\dot{\gamma}) = k\dot{\gamma}^{n-1}$.

References and Notes

(1) Keller, A.; Kolnaar, H. W., Flow-induced orientation and structure formation. In *Materials Science and Technology, Processing of Polymers*; Meijer, H. E. M., Ed.; Wiley-VCH: New York, 1997; pp 189−268.
(2) Mykhaylyk, O. O.; Chambon, P.; Graham, R. S.; Fairclough, J. P. A.; Olmsted, P. D.; Ryan, A. J. *Macromolecules* **2008**, *41*, 1901–1904.
(3) Eder, G.; Janeschitz-Kriegl, H.; Liedauer, S. *Prog. Polym. Sci.* **1990**, *15*, 629–714.
(4) Janeschitz-Kriegl, H.; Ratajski, E.; Stadlbauer, M. *Rheol. Acta* **2003**, *42*, 355–364.
(5) Janeschitz-Kriegl, H.; Ratajski, E. *Polymer* **2005**, *46*, 3856–3870.
(6) Larson, M. A.; Garside, J. *J. Cryst. Growth* **1986**, *76* (1), 88–92.
(7) Larson, M. A.; Garside, J. *Chem. Eng. Sci.* **1986**, *41*, 1285–1289.
(8) Becker, R.; Doring, W. *Ann. Phys.* **1935**, *24*, 719–752.
(9) van Meerveld, J.; Peters, G. W. M.; Hutter, M. *Rheol. Acta* **2004**, *44*, 119–134.
(10) Janeschitz-Kriegl, H.; Eder, G. *Journal of Macromolecular Science Part B-Physics* **2007**, *46*, 591–601.
(11) Housmans, J. W.; Steenbakkers, R. J. A.; Roozemond, P. C.; Peters, G. W. M.; Meijer, H. E. H. *Macromolecules* **2009**, *42*, 5728–5740.
(12) Gibbs, J. W. *The Scientific Papers of J. Willard Gibbs*; Dover Publications: New York, 1961; Vol. *1*, p 434.
(13) Coppola, S.; Grizzuti, N.; Maffettone, P. L. *Macromolecules* **2001**, *34*, 5030–5036.
(14) Stadlbauer, M.; Janeschitz-Kriegl, H.; Eder, G.; Ratajski, E. *J. Rheol.* **2004**, *48*, 631–639.
(15) Caputo, F. E.; Burghardt, W. R. *Macromolecules* **2001**, *34*, 6684–6694.
(16) Baert, J.; Van Puyvelde, P.; Langouche, F. *Macromolecules* **2006**, *39*, 9215–9222.
(17) Kumaraswamy, G.; Verma, R. K.; Kornfield, J. A. *Rev. Sci. Instrum.* **1999**, *70*, 2097–2104.
(18) Liedauer, S.; Eder, G.; Janeschitz-Kriegl, H.; Jerschow, P.; Geymayer, W.; Ingolic, E. *Int. Polym. Process.* **1993**, *8* (3), 236–244.
(19) Nogales, A.; Hsiao, B. S.; Somani, R. H.; Srinivas, S.; Tsou, A. H.; Balta-Calleja, F. J.; Ezquerra, T. A. *Polymer* **2001**, *42*, 5247–5256.
(20) Macosko, C. W. *Rheology: principles, measurements, and applications*; VCH Publishers, Inc.: New York, 1994; p 568.
(21) Fernandez-Ballester, L.; Thurman, D. W.; Kornfield, J. A. *J. Rheol.* **2009**, *53*, 1229–1254.
(22) Kumaraswamy, G.; Verma, R. K.; Kornfield, J. A.; Yeh, F. J.; Hsiao, B. S. *Macromolecules* **2004**, *37*, 9005–9017.
(23) Heeley, E. L.; Morgovan, A. C.; Bras, W.; Dolbnya, I. P.; Gleeson, A. J.; Ryan, A. J. *Physchemcomm* **2002**, 158–160.
(24) Keum, J. K.; Zuo, F.; Hsiao, B. S. *Macromolecules* **2008**, *41*, 4766–4776.
(25) Ogino, Y.; Fukushima, H.; Takahashi, N.; Matsuba, G.; Nishida, K.; Kanaya, T. *Macromolecules* **2006**, *39*, 7617–7625.
(26) Somani, R. H.; Hsiao, B. S.; Nogales, A.; Srinivas, S.; Tsou, A. H.; Sics, I.; Balta-Calleja, F. J.; Ezquerra, T. A. *Macromolecules* **2000**, *33*, 9385–9394.
(27) Sutton, D.; Hanley, T.; Knott, R.; Cookson, D. *J. Synchrotron Radiat.* **2004**, *11*, 505–507.
(28) Janeschitz-Kriegl, H. *Monatsh. Chem.* **2007**, *138* (4), 327–335.
(29) Marand, H.; Xu, J. N.; Srinivas, S. *Macromolecules* **1998**, *31*, 8219–8229.
(30) Xu, J. N.; Srinivas, S.; Marand, H.; Agarwal, P. *Macromolecules* **1998**, *31*, 8230–8242.
(31) Wunderlich, B. *J. Appl. Polym. Sci.* **2007**, *105* (1), 49–59.
(32) Bloss, F. D. *Optical Crystallography*; Mineralogical Society of America: Washington DC, 1999; p 239.
(33) Hosier, I. L.; Alamo, R. G.; Esteso, P.; Isasi, J. R.; Mandelkern, L. *Macromolecules* **2003**, *36*, 5623–5636.
(34) Auriemma, F.; De Rosa, C.; Boscato, T.; Corradini, P. *Macromolecules* **2001**, *34*, 4815–4826.
(35) Keith, H. D.; Padden, F. J. *J. Polym. Sci.* **1958**, *31*, 415–421.

(36) Janeschitz-Kriegl, H. *Polymer Melt Rheology and Flow Birefringence*; Springer-Verlag: Berlin, 1983; p 524.
(37) Kawaguchi, K. *J. Appl. Polym. Sci.* **2006**, *100* (4), 3382–3392.
(38) Saville, B. P., Polarized Light: Qualitative Microscopy. In *Applied Polymer Light Microscopy*, Hemsley, D. A., Ed. Alsevier Applied Science: London, 1989; pp 111−149.
(39) Morrison, F. A., Steady shear flow. In *Understanding Rheology*: Oxford University Press: Oxford, 2001; pp 169−190.
(40) Heeley, E. L.; Fernyhough, C. M.; Graham, R. S.; Olmsted, P. D.; Inkson, N. J.; Embery, J.; Groves, D. J.; McLeish, T. C. B.; Morgovan, A. C.; Meneau, F.; Bras, W.; Ryan, A. J. *Macromolecules* **2006**, *39*, 5058–5071.
(41) Hsiao, B. S., Role of Chain Entanglement Network on Formation of Flow-Induced Crystallization Precursor Structure. In *Progress in Understanding of Polymer Crystallization*; Reiter, G., Strobl, G. R., Eds.; Springer: Berlin, 2007; pp 131−149.
(42) Groisman, A.; Steinberg, V. *Nature* **2000**, *405* (6782), 53–55.
(43) Schiamberg, B. A.; Shereda, L. T.; Hu, H.; Larson, R. G. *J. Fluid Mech.* **2006**, *554*, 191–216.
(44) Tadmor, Z.; Gogos, C. G., *Principles of Polymer Processing*, 2nd ed.; John Wiley & Sons: New York, 2006; p 962.
(45) Van Krevelen, D. W. *Properties of Polymers*; Elsevier: Amsterdam, 1990; p 475.
(46) Shin, Y. W.; Uozumi, T.; Terano, M.; Nitta, K. H. *Polymer* **2001**, *42*, 9611–9615.
(47) Fernyhough, C. M.; Young, R. N.; Poche, D.; Degroot, A. W.; Bosscher, F. *Macromolecules* **2001**, *34*, 7034–7041.
(48) Cross, M. M. *J. Colloid Sci.* **1965**, *20*, 417–437.